

OAK RIDGE NATIONAL LABORATORY

operated by

UNION CARBIDE CORPORATION

for the

U.S. ATOMIC ENERGY COMMISSION



ORNL-TM-405

ey-11

THERMAL FATIGUE - AN ANALYSIS OF THE EXPERIMENTAL METHOD

A. E. Carden

NOTICE

This document contains information of a preliminary nature and was prepared primarily for internal use at the Oak Ridge National Laboratory. It is subject to revision or correction and therefore does not represent a final report. The information is not to be abstracted, reprinted or otherwise given public dissemination without the approval of the ORNL patent branch, Legal and Information Control Department.

LEGAL NOTICE

This report was prepared as an account of Government sponsored work. Neither the United States, nor the Commission, nor any person acting on behalf of the Commission:

- A. Makes any warranty or representation, expressed or implied, with respect to the accuracy, completeness, or usefulness of the information contained in this report, or that the use of any information, apparatus, method, or process disclosed in this report may not infringe privately owned rights; or
- B. Assumes any liabilities with respect to the use of, or for damages resulting from the use of any information, apparatus, method, or process disclosed in this report.

As used in the above, "person acting on behalf of the Commission" includes any employee or contractor of the Commission, or employee of such contractor, to the extent that such employee or contractor of the Commission, or employee of such contractor prepares, disseminates, or provides access to, any information pursuant to his employment or contract with the Commission, or his employment with such contractor.

ORNL-TM-405

Copy

Contract No. W-7405-eng-26

Metals and Ceramics Division

THERMAL FATIGUE - AN ANALYSIS OF THE EXPERIMENTAL METHOD

A. E. Carden

DATE ISSUED

JAN - 4 1963

OAK RIDGE NATIONAL LABORATORY
Oak Ridge, Tennessee
operated by
UNION CARBIDE CORPORATION
for the
U. S. ATOMIC ENERGY COMMISSION



TABLE OF CONTENTS

ABSTRACT -----	1
INTRODUCTION -----	1
TYPES OF FATIGUE EXPERIMENTS -----	4
General -----	4
Isothermal Strain-Fatigue Tests -----	6
Thermal-Fatigue Tests -----	7
ANALYSIS OF THE THERMAL-FATIGUE TEST -----	7
Simplified Case -----	7
General -----	7
Method I -----	11
Method II -----	12
Method III -----	12
The P-T Loop of the Model -----	13
Plastic-Strain Energy from the P-T Loop -----	15
Actual Case -----	15
General -----	17
Significance of Lengths L_1 and L_2 -----	17
Method I, Eq. (10) -----	21
Method II, Eq. (13) -----	22
Method III, Eq. (18) -----	22
Discussion of Geometric Stability -----	23
Constancy of Parameters -----	28
Temperature Profiles -----	28
Actual P-T Loop -----	28
The Stress-Strain Diagram -----	31
ALTERNATE TEST METHODS -----	37
Segmented-Type Tubular Test Specimen -----	37
Servocontrolled Testing Machines -----	37
An Alternate Thermal-Fatigue Test -----	38
SUMMARY -----	43
ACKNOWLEDGMENTS -----	44
APPENDIX A -----	45
Description of the Conventional Thermal-Fatigue Test -----	47
Discussion of the Major Difficulties of the Thermal-Fatigue Test -----	54
APPENDIX B -----	57
Nomenclature -----	59
Subscripts -----	59
Superscripts -----	59
APPENDIX C -----	61
Required Test Information for the Thermal-Fatigue Test -----	63

THERMAL FATIGUE - AN ANALYSIS OF THE EXPERIMENTAL METHOD

A. E. Carden*

ABSTRACT

An analysis of the conventional (Coffin-type) thermal-fatigue test is presented by describing an analytical model from which three methods for determining the plastic-strain range are derived. One of the methods for calculating the plastic strain does not require the knowledge or use of the thermal coefficient, modulus of elasticity, or stress range. The accuracy of this method is not affected by the variation of the thermal coefficient, modulus of elasticity, or yield strength during the heating and cooling periods. Plastic strains resulting from yielding and relaxation may be accounted for by this method. The errors of conventional methods are discussed. A method for plotting the stress-strain hysteresis loop is also given.

From an analysis of the load-temperature loop, it is clearly shown how all of the significant variables can be determined without plotting a stress-strain hysteresis loop. The plastic-strain range, the mechanical-strain range (elastic plus plastic), the stress range, and the plastic-strain energy per cycle can easily be determined from the load-temperature loop.

An alternate test is suggested that minimizes all of the major difficulties of the conventional test. An improved test specimen for the conventional test is also recommended.

INTRODUCTION

The volume of a solid body increases or expands when the temperature of that body is raised. This change of volume is called "thermal expansion," and the term "thermal strain" refers to the unit change of a lineal dimension that is associated with the rise in temperature. No internal stress is produced in a solid material if the temperature increase is the same in all parts of the body and if the volume change is unrestrained.

*Summer employee.

In a solid that is restrained so that it cannot expand (or contract) freely, a temperature change gives rise to a stress called a "thermal stress." A mechanical deformation is uniquely related to and concurrent with a thermal stress. A thermal-stress deformation that is recovered or relieved when the restraint is removed is said to be an elastic deformation. A thermal-stress deformation that is not recovered when the restraint is removed is said to be a plastic deformation. Plastic deformations can result from large thermal stresses, high temperatures, or long duration of stress application.

The elastic and plastic deformation together constitute the internal, or mechanical-load, strain which hereafter will be referred to simply as mechanical strain. The mechanical strain at a point is always related to the stress at that point and this stress can be produced independent of temperature. A mechanical strain is not uniquely dependent on temperature, but a thermal strain is. A thermal strain can occur without producing a thermal stress (i.e., in an unrestrained body), but a thermally induced stress (in a restrained body) always produces or is accompanied by a mechanical strain.

In thermal-fatigue tests there are, therefore, three kinds of strain: thermal strain, mechanical strain, and geometric strain. A thermal strain is that strain produced by temperature change. A mechanical strain is that strain which is produced by a stress, and there is no intrinsic difference between a thermal stress and a mechanical stress. A geometric strain is that which can be physically measured by a displacement. The geometric, or observed, strain is the algebraic sum of the mechanical strain and the thermal strain.

A repeated fluctuation of temperature in a restrained solid produces cyclic thermal stresses (and strain), leading ultimately to failure. The name "thermal fatigue" is applied to failures produced by cyclic thermal stresses. The cyclic mechanical strains associated with the thermal stresses may be only elastic, or they may contain both elastic and plastic components. The significant variables for thermal fatigue are stress, time, mechanical strain (or frequently the plastic-strain component), and temperature range.

The conventional thermal-fatigue experiment can be simply described as the alternate heating and cooling of a thin-walled tubular specimen in a device that restricts the longitudinal movement of the specimen.

A timely and significant critical review of the subject of thermal fatigue by T. C. Yen¹ has recently been published. The review is primarily an appraisal of some of the significant results of thermal-fatigue experiments. The article includes a brief discussion of the test method and summarizes the two major difficulties of the conventional thermal-fatigue test: (1) the lack of a uniform temperature throughout the length of a tubular specimen and (2) the measurement of the mechanical strain, especially the plastic component, produced by restrained thermal cycling.

For several years thermal-fatigue testing was pursued with vigor and gained widespread attention. Interest abated, however, when apparent lack of success met efforts to obtain good agreement between the experimental results and the lives of service applications, or between thermal-fatigue and isothermal strain-fatigue data. No satisfactory explanation of the dilemma was universally accepted, and a shadow of doubt began to cloud the experimental method.

The value of the thermal-fatigue test has been contested by critics because many believe that the published methods of determining the plastic-strain values are questionable, that any calculated value of plastic strain may be gravely in error, that the construction of a stress-strain diagram is not possible, and that the plastic strain per cycle indeed becomes an illusive quantity to calculate. The reasons for doubting the validity of the results of the conventional test have not rested simply on prejudice. The thermal coefficient, modulus of elasticity, and strength properties all vary with temperature, which in this test varies with time. Too, the temperature at any instant of time varies throughout the length of the specimen. Thus the problem has appeared to be too complex to deduce the stress-strain cycle of the material.

¹T. C. Yen, "Thermal Fatigue - A Critical Review," Welding Res. Council Bull. S., No. 72 (October 1961).

Thermal-fatigue reports often do not relate how the plastic-strain values were calculated and are vague about how other data were obtained. A clear, critical analysis of the published methods of determining the plastic strain has not yet appeared. The possible reasons why thermal-fatigue data do not always show good agreement with isothermal strain-fatigue results are generally not discussed. A need exists to extend Yen's review to analyze the experimental problem and to suggest possible alternatives.

The purpose of this paper is to present a simplified model of the thermal-fatigue test. Using this model, a method is developed for determining the stress-strain cycle, and three techniques for calculating the magnitude of the plastic strain are presented. The possible errors of these methods are discussed. It will be demonstrated how one method answers, in part, several of the basic problems of the conventional experiment.

A second purpose of this paper is to propose a modification of the thermal-fatigue test that will minimize other deficiencies of the prevalent experimental method.

TYPES OF FATIGUE EXPERIMENTS

General

Fatigue experiments are conventionally conducted by alternating one of three parameters in a test coupon until failure occurs. The stress, strain, or temperature can be programmed to vary with time, as shown in Fig. 1, to produce the appropriate stress-strain or stress-temperature cycle.

For cyclic loading under conditions of elastic behavior, only a single line exists on a stress-strain diagram; the loading and unloading paths are identical. Stress is usually the significant variable in the elastic region of cyclic loading.

For low-cycle or high-stress fatigue of ductile materials, the important variable is strain, and perhaps more precisely, the plastic strain. Moreover, empirical equations can be deduced from laboratory tests that describe the fatigue behavior of the material under a specified set of conditions of cyclic strain. The term "isothermal

UNCLASSIFIED
ORNL-LR-DWG 71547

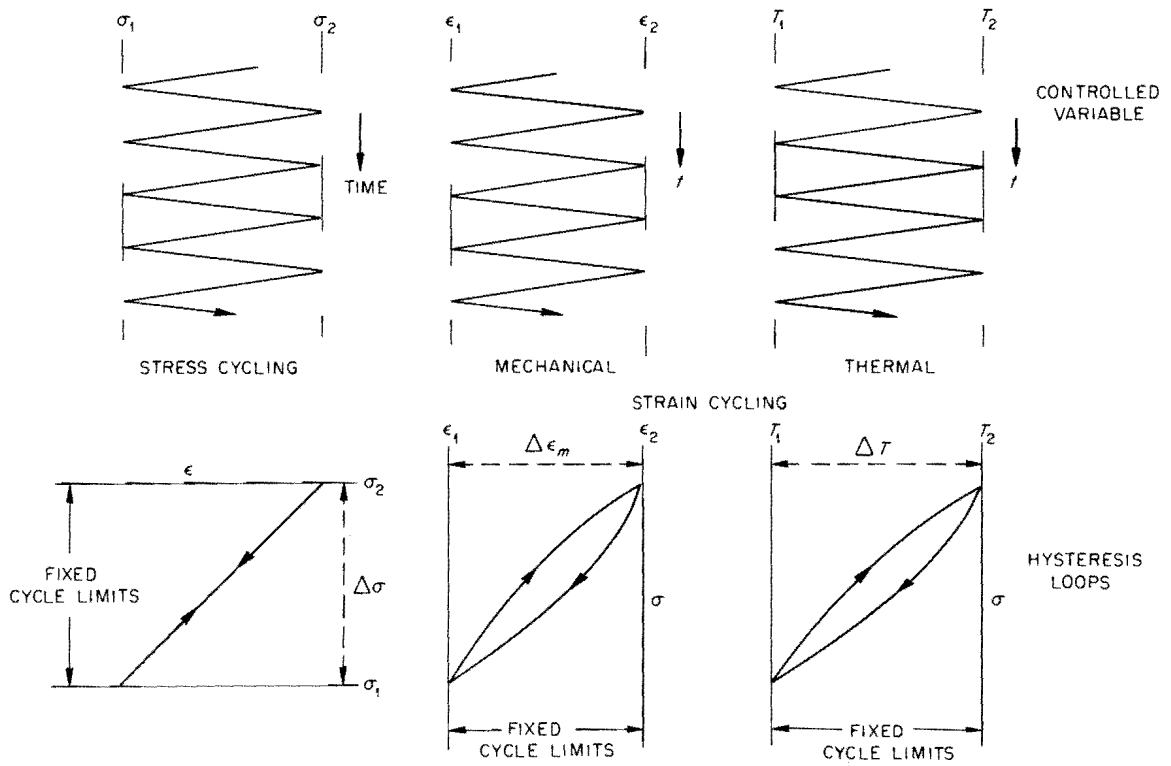


Fig. 1. Three Types of Fatigue Tests.

strain fatigue" is applied to tests in which the temperature is constant and the mechanical strain is the programmed variable. In the thermal-fatigue test, sometimes referred to as the thermal-strain cycling test, temperature is the programmed variable. Two important questions are: (1) Are the results of isothermal-strain fatigue and thermal-fatigue tests equal, related, or incomparable? (2) How is the resistance to thermal fatigue best analyzed? Before reliable answers are obtained to these questions, it must be determined if the parameters of the thermal-fatigue experiment are accurately known and if the variations of parameters in a laboratory thermal-fatigue test are comparable to the conditions of the service application.

Isothermal Strain-Fatigue Tests

Because the conventional thermal-fatigue test has been so highly criticized and the tendency has become so widespread to apply isothermal-fatigue results to thermal-fatigue problems, one would think that the isothermal-fatigue test is free from difficulties and approximations. Usually a mechanical device cycles the specimen between two fixed extension limits while a separate controller maintains a constant temperature in the specimen. The plastic strain in the sample is generally not measured directly and often the plastic strain is not distributed uniformly. For large values of cyclic strain, the specimen often buckles. Several of the problems of this test are discussed in an Appendix of Reference 2, and detailed descriptions of isothermal strain-fatigue test apparatus can be found in the literature.²⁻⁷

²R. W. Swindeman, Strain-Fatigue Properties of Inconel. Part II. Isothermal Tests with Constant Hold Time, ORNL-3250 (March 29, 1962).

³R. W. Swindeman and D. A. Douglas, Jr., Trans. ASME, Ser. D: J. Basic Eng. 81, 203-08 (1959) Paper No. 58-A-198.

⁴W. R. Anderson and C. R. Waldron, High Temperature-Strain Fatigue Testing with a Modified Direct-Stress Fatigue Machine, NAA-SR-4051 (1959).

⁵C. A. Johansson, "Fatigue of Steels at Constant Strain Amplitude and Elevated Temperature," p 112 in International Union of Theoretical and Applied Mechanics. Colloquium on Fatigue, Stockholm, May 25-27, 1955, ed. by Waloddi Weibull, Springer/Verlag, Berlin, 1956.

⁶W. N. Findley, ASTM Bull. No. 147, 54-6 (August 1947).

⁷E. E. Baldwin, G. J. Sokol, and L. F. Coffin, Jr., Am. Soc. Testing Mater., Proc. 57, 567-81 (1957).

Thermal-Fatigue Tests

In the conventional thermal-fatigue test, a thin-walled tubular sample is alternately heated and cooled in an apparatus that restricts the longitudinal thermal movement of the specimen. The straight portion of the specimen length is commonly 2 in. and at each end of the gage length are two fillets that constitute about one third of the total length. Usually a large electric current passing through the specimen is the heat source and a stream of compressed gas passing through the central hole cools the sample. The axial load is determined from two load cells that restrain the thermal movement of the specimen. Because the restraint system is not perfectly rigid, a dial gage measures the small displacement of the specimen ends during restrained cycling. Due to the heat sink at each end of the specimen, the temperature throughout the length is never uniform. The problems of directly gaging the strain during thermal cycling are complex. The determination of the stress-strain cycle becomes one of deduction. The temperature of the midlength of the specimen, the axial load, and the displacement of the ends of the sample are generally the only measurements available. For the reader who is not familiar with the conventional test, a detailed description of the thermal-fatigue test and a discussion of the deficiencies of the test are included in Appendix A.

ANALYSIS OF THE THERMAL-FATIGUE TEST

Simplified Case

The methods to be presented for calculating the value of the plastic-strain range are based on a simplified model of the typical thermal-fatigue test. The nomenclature for this model is defined in Appendix B. The necessity for each of the details of this model will be discussed when the model is compared to the actual case.

General

The reader should study the details of the graphical representation of this model shown in Figs. 2 and 3. The specimen consists of two segments, each having uniform but unequal cross-sectional areas designated by appropriate subscripts. This specimen is uniformly

UNCLASSIFIED
ORNL-LR-DWG 71551

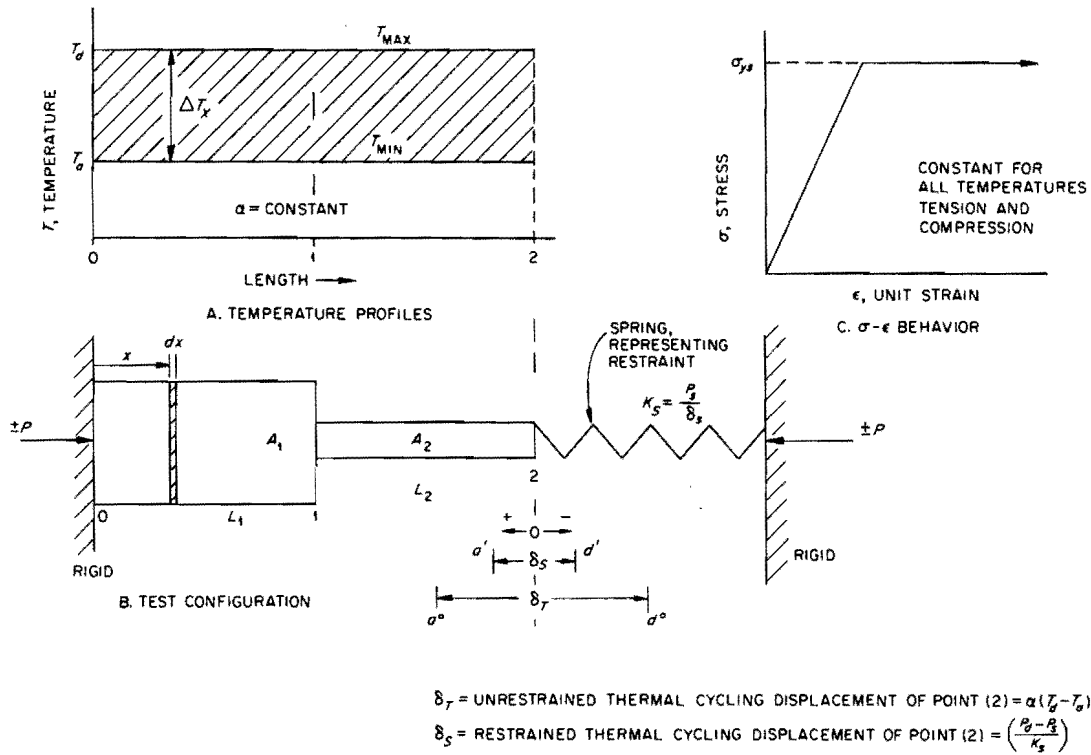


Fig. 2. Model of Conventional Thermal-Fatigue Test.

UNCLASSIFIED
ORNL-LR-DWG 71553

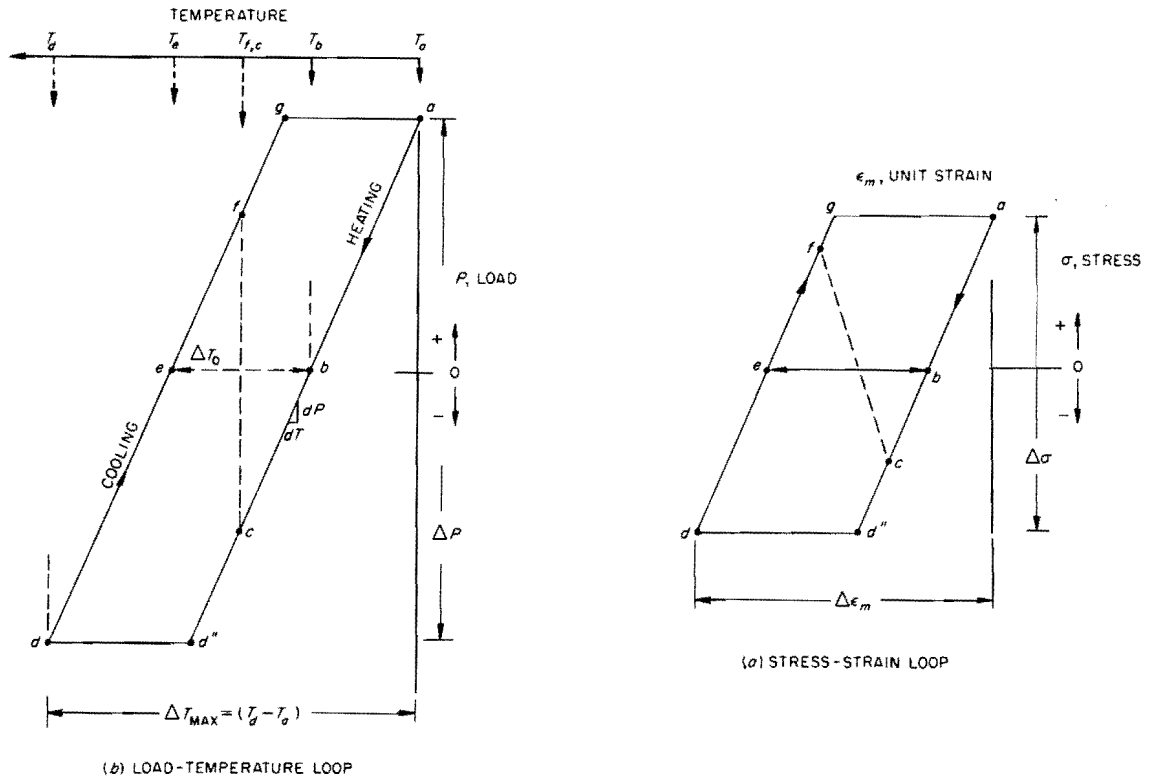


Fig. 3. Hysteresis Loops for Area A₂ for Thermal-Fatigue Model.

cycled between the temperatures T_a and T_d and has an elasto-plastic mechanical behavior. The thermal coefficient of expansion α is constant. The specimen is anchored to a rigid end at section (0) and is attached at section (2) to a spring having a constant, K_s . With the spring removed, the geometric displacement of point (2) during the temperature rise from (a) to (d) is

$$\delta_T = \int_0^2 \int_a^d \alpha (dT)(dx) . \quad (1)$$

The displacement δ_T is equal to the area between temperature profiles multiplied by α . Since ΔT_x is a constant over the length (0-2) and α is constant, the total thermal strain is

$$\delta_T = \alpha (T_d - T_a)(L_1 + L_2) . \quad (2)$$

The specimen is heated to an intermediate temperature between T_a and T_d and the spring is attached such that zero load exists in the specimen. A geometric displacement of point (2) is observed as the temperature cycles. This displacement is also deflection δ_s of the spring, and

$$\delta_s = \frac{P_a - P_d}{K_s} . \quad (3)$$

The difference of these two displacements δ_T and δ_s is therefore the total mechanical strain sustained by the specimen as a result of the change in load ($P_a - P_d$). This mechanical strain δ_m produced by the loading effect of the restraint is the sum of the elastic and plastic components.

$$\delta_m = \int_0^2 \epsilon_e (dx) + \int_0^2 \epsilon_p (dx) , \quad (4)$$

and it is clear that

$$\delta_m = \delta_T - \delta_s . \quad (5)$$

Because the temperature is uniform at any time t , a plot of temperature vs load will produce a loop resembling that shown in Fig. 3a. The total mechanical strain during an increment of change in temperature T_a to T_b is

$$\delta_m \Big|_a^b = \delta_T \Big|_a^b - \epsilon_s \Big|_a^b \quad (6)$$

$$\delta_m \Big|_a^b = \alpha (T_b - T_a)(L_1 + L_2) - \frac{P_b - P_a}{K_s} \quad (7)$$

From the P-T loop, any one of several methods can now be employed to determine the plastic-strain range $\Delta\epsilon_p$ without plotting the stress-strain curve. The plastic-strain range is equal to the maximum internal width of the stress-strain loop shown in Fig. 3b and is sometimes called the plastic strain per half cycle.

Method I. - The total plastic strain per half cycle $\Delta\delta_p$ is equal to the residual mechanical strain after the excursion of heating and cooling for the half cycle (b-c-d''-d-e). This plastic strain is the strain that remains in the sample after heating from zero load (point b) to T_{max} (point d) and cooling to zero load (point e). From Eq. (7) the total plastic strain per half cycle is

$$\Delta\delta_p = \delta_m \Big|_b^e = \alpha (T_e - T_b)(L_1 + L_2) - \frac{P_b - P_e}{K_s} \quad (8)$$

Since $P_b = P_e = 0$,

$$\Delta\delta_p = \alpha (T_e - T_b)(L_1 + L_2) \quad (9)$$

Because the length L_2 is reduced in cross section and the material is elasto-plastic, yielding will occur only in the length L_2 . The unit plastic-strain range in the length L_2 is

$$\Delta\epsilon_p = \alpha (T_b - T_e) \left(\frac{L_1 + L_2}{L_2} \right) \quad (10)$$

The significance of Eq. (10) is that the width of the load-temperature loop at zero load is directly related to the plastic-strain range. The value $(L_1 + L_2)$ is the total length that contributes to the thermal

displacement of the specimen, and L_2 is the only length that sustains plastic flow. That the length sustaining plastic flow is not equal to the length undergoing cyclic thermal expansion is noteworthy.

Method II. - The plastic-strain range can also be computed by calculating the mechanical strain from the minimum temperature (point a) to the maximum temperature (point d) and subtracting the elastic strain component. The total mechanical strain from Eq. (4) is the sum of the elastic and plastic components, or

$$\delta_e + \delta_p = \delta_T - \delta_s, \quad (11)$$

or

$$\delta_p = \alpha (\Delta T) (L_1 + L_2) - \frac{\Delta P}{K_s} - \frac{\Delta P}{E} \left(\frac{L_1}{A_1} + \frac{L_2}{A_2} \right). \quad (12)$$

Since $\delta_p = \epsilon_p L_2$, then

$$\Delta \epsilon_p = \alpha (\Delta T) \left(\frac{L_1 + L_2}{L_2} \right) - \frac{\Delta P}{K_s L_2} - \frac{\Delta P}{E L_2} \left(\frac{L_1}{A_1} + \frac{L_2}{A_2} \right). \quad (13)$$

If the ratio $\frac{L_1}{A_1}$ is much less than $\frac{L_2}{A_2}$, then

$$\Delta \epsilon_p \approx \alpha (\Delta T) \left(\frac{L_1 + L_2}{L_2} \right) - \frac{\Delta \sigma_2}{E} - \frac{\Delta P}{K_s L_2}. \quad (14)$$

In Eqs. (12-14) ΔT , ΔP , and $\Delta \sigma$ are the range of values and equal to the maximum minus the minimum value. Equation (13) clearly shows the influence of the specimen geometry and of the elasticity of the restraint on the magnitude of $\Delta \epsilon_p$.

Method III. - If a constant temperature line through the loop of Fig. 3a intersects the elastic (linear) portion of both the heating and cooling regions (points c and f, respectively), then only the difference in load is required to calculate the plastic-strain range.

Since $\delta_m = \delta_T - \delta_s$, then

$$\delta_m \Big|_c^f = \alpha (T_f - T_c) (L_1 + L_2) - \frac{P_f - P_c}{K_s}. \quad (15)$$

But $T_c = T_f$; therefore,

$$\delta_m \Big|_c^f = - \frac{P_f - P_c}{K_s} , \quad (16)$$

or

$$\delta_p \Big|_c^f = - \frac{P_f - P_c}{K_s} - \frac{P_f - P_c}{E} \left(\frac{L_1}{A_1} + \frac{L_2}{A_2} \right) , \quad (17)$$

or

$$\Delta \epsilon_p = - \frac{P_f - P_c}{L_2} \left(\frac{L_1}{A_1 E} + \frac{L_2}{A_2 E} + \frac{1}{K_s} \right) . \quad (18)$$

Again, if $\frac{L_1}{A_1} \ll \frac{L_2}{A_2}$, then

$$\Delta \epsilon_p \approx - \frac{\Delta P}{K_s L_2} \Big|_c^f - \frac{\Delta \sigma_2}{E} \Big|_c^f . \quad (19)$$

The P-T Loop of the Model

A slight digression may be of benefit at this point to extend the analysis of the load-temperature (P-T) loop in order to determine the slope of the P-T curve $\frac{dP}{dT}$ at zero load. At zero load the increment of plastic strain is zero for a small increment of load and the mechanical strain is only elastic. Since $\delta_m = \delta_T - \delta_s$ and δ_m is only

$\left(\frac{PL}{AE} \right)_1 + \left(\frac{PL}{AE} \right)_2$, then an infinitesimal increment of δ_m accompanying

an increment of temperature change dT may be written as

$$dP \left(\frac{L_1}{A_1 E} + \frac{L_2}{A_2 E} \right) = \alpha dT (L_1 + L_2) - \frac{dP}{K_s} , \quad (20)$$

or

$$dP \left(\frac{L_1}{A_1 E} + \frac{L_2}{A_2 E} + \frac{1}{K_s} \right) = \alpha dT (L_1 + L_2) , \quad (21)$$

and

$$\frac{dP}{dT} \Big|_{P=0} = \frac{\alpha(L_1 + L_2)}{\left(\frac{L_1}{A_1 E} + \frac{L_2}{A_2 E} + \frac{1}{K_s} \right)} . \quad (22)$$

The slope of the P-T loop at zero load is a function of α , E, K_s , and the lengths and areas of the segmented specimen.

If perfect rigidity were attainable, the term $\frac{1}{K_s}$ would drop out.

By substitution of typical values into Eq. (22), it can be shown that about one third of the slope of P vs T stems from the term $\frac{1}{K_s}$. Thus,

it is indicated that the deflection of the constraint system must be considered in the methods presented.

The fact that the constraint system has an appreciable deflection and that δ_m will always be less than δ_T does not imply that the mechanical strain range $\Delta\epsilon_m$ is always less than $\alpha\Delta T$; indeed, $\Delta\epsilon_m$ is usually greater than $\alpha\Delta T$. From $\delta_m = \delta_T - \delta_s$ it follows that

$$\epsilon_{m1} L_1 + \epsilon_{m2} L_2 = \alpha\Delta T (L_1 + L_2) - \frac{\Delta P}{K_s} \quad , \quad (23)$$

and

$$\epsilon_{m2} L_2 = \alpha\Delta T (L_1 + L_2) - \frac{\Delta P}{K_s} - \frac{\Delta P}{E} \left(\frac{L_1}{A_1} \right) \quad , \quad (24)$$

or

$$\epsilon_{m2} = \alpha\Delta T \left(\frac{L_1 + L_2}{L_2} \right) - \frac{\Delta P}{L_2} \left(\frac{1}{K_s} + \frac{L_1}{A_1 E} \right) \quad . \quad (25)$$

In other words, the mechanical strain in length L_2 is greater than $\alpha(\Delta T)$ provided that the negative term of Eq. (25) does not nullify the effects of the factor $\left(\frac{L_1 + L_2}{L_2} \right)$ which is always greater than one; i.e.,

if

$$\Delta P \left(\frac{1}{K_s} + \frac{L_1}{A_1 E} \right) \leq L_1 \alpha\Delta T \quad . \quad (26)$$

Some have described or defined the ratio of $\frac{\delta_m}{\delta_T}$ as a measure of

the degree of constraint. This ratio is always less than one. It would be far better to define the degree of constraint by the ratio of $\frac{\Delta\epsilon_m}{\alpha(\Delta T)}$. This ratio of the unit mechanical strain during some

excursion of temperature ΔT to the value of uninhibited thermal strain over the same temperature range is usually greater than one. The degree of constraint is represented by the factor F. The mechanical-strain range is therefore equal to uninhibited thermal strain

$\alpha(\Delta T)_{\max}$ times the factor F. The factor F is dependent on the lengths and areas of the specimen E and K_s .

Plastic-Strain Energy from the P-T Loop. - The increment of total-strain energy dW put into the system during the increment of temperature change dT of Fig. 4 is $P \cdot d(\delta_m)$. The mechanical strain may be obtained from Eq. (5), and $dE = P \cdot d(\delta_T - \delta_s)$, or

$$dW = P\alpha (dT)(L_1 + L_2) - \frac{P(dP)}{K_s} . \quad (27)$$

The change of strain energy from e to a is

$$W_a - W_e = \alpha (L_1 + L_2) \int_e^a P (dT) - \frac{1}{K_s} \int_e^a P (dP) . \quad (28)$$

The recovered energy on unloading is

$$W_a - W_b = \alpha (L_1 + L_2) \int_a^b P (dT) - \frac{1}{K_s} \int_a^b P (dP) . \quad (29)$$

The energy dissipated during the half cycle e-a-b is one half of the total plastic-strain energy per cycle and is

$$\frac{\Delta W_p}{2} = \alpha (L_1 + L_2) \left[\int_e^a P (dT) - \int_a^b P (dt) \right] . \quad (30)$$

The total plastic-strain energy per cycle is therefore the area contained within the P-T loop multiplied by $(\alpha)(L_1 + L_2)$.

Actual Case

In order to apply the simplified analysis to the actual experiment, one needs to recall the assumptions of that development. It was assumed that there were two distinct lengths having different areas. The plastic strain was assumed to be uniformly distributed in length L_2 , and the temperature was independent of length. The material properties were independent of temperature and the material was elasto-plastic.

UNCLASSIFIED
ORNL-LR-DWG 71554

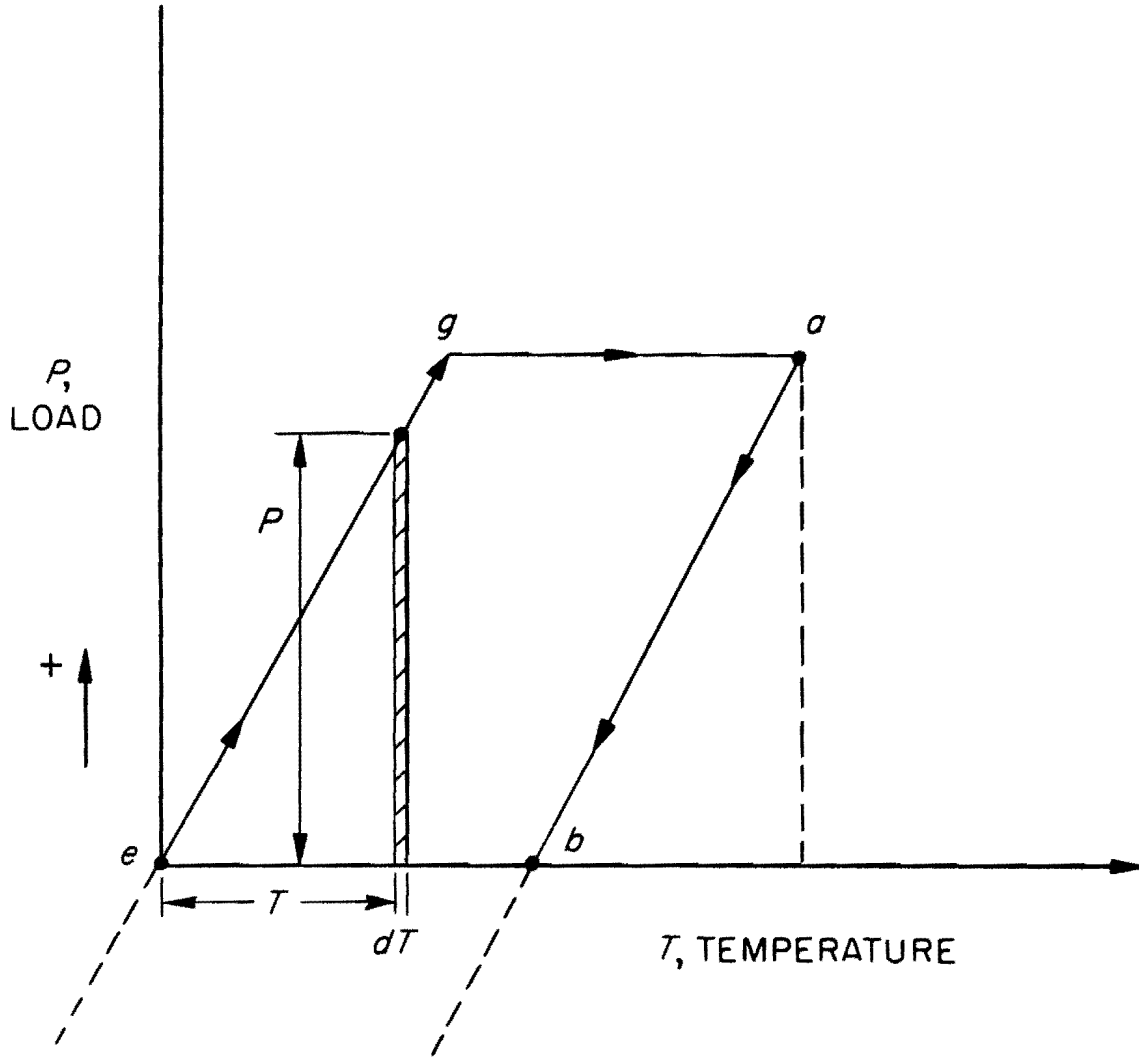


Fig. 4. Tensile Portion of Load-Temperature Loop.

General

A typical thermal-fatigue specimen is shown in Fig. 5 with the measured temperature profiles at the maximum and minimum temperatures. The total unrestrained thermal movement δ_T may be measured with a suitable transducer and is equal to the area between the profiles multiplied by α .

$$\delta_T = \int_0^L \int_{T_{\min}}^{T_{\max}} \alpha (\Delta T)_x dx \quad . \quad (31)$$

Wyatt and Jordan⁸ have experimentally verified this equation in numerous tests.

For the specimen shown in Fig. 5, the total mechanical-strain range obtained from Eq. (5) is

$$\Delta\delta_m = \int_0^L \int_{T_1}^{T_2} \alpha (\Delta T_x) dx - \frac{\Delta P}{K_s} \quad . \quad (32)$$

The value $\frac{P}{K_s}$ is equal to δ_s and is the deflection of the restraint system. The values of δ_T and δ_s are commonly measured with a dial gage. One is not free to neglect δ_s as being insignificant. The deflection of the restraint constitutes an appreciable unloading effect, thereby making it absolutely necessary that the model contain an element that represents an elastic restraint.

Significance of Lengths L_1 and L_2 . - An effective gage length L° is determined from the change of a dial gage reading ΔD° during unrestrained thermal cycling. Thus, ΔD° is analogous to the unrestrained displacement of the ends of the model specimen of total length L heated uniformly from T_a to T_d ,

$$\Delta D^\circ = \alpha (T_d - T_a) L \quad . \quad (33)$$

⁸A. E. Wyatt and W. D. Jordan, "Temperature Distribution Studies: Memo Report No. 5," Bureau of Engineering Research, University of Alabama (May 1957).

UNCLASSIFIED
ORNL-LR-DWG 71552

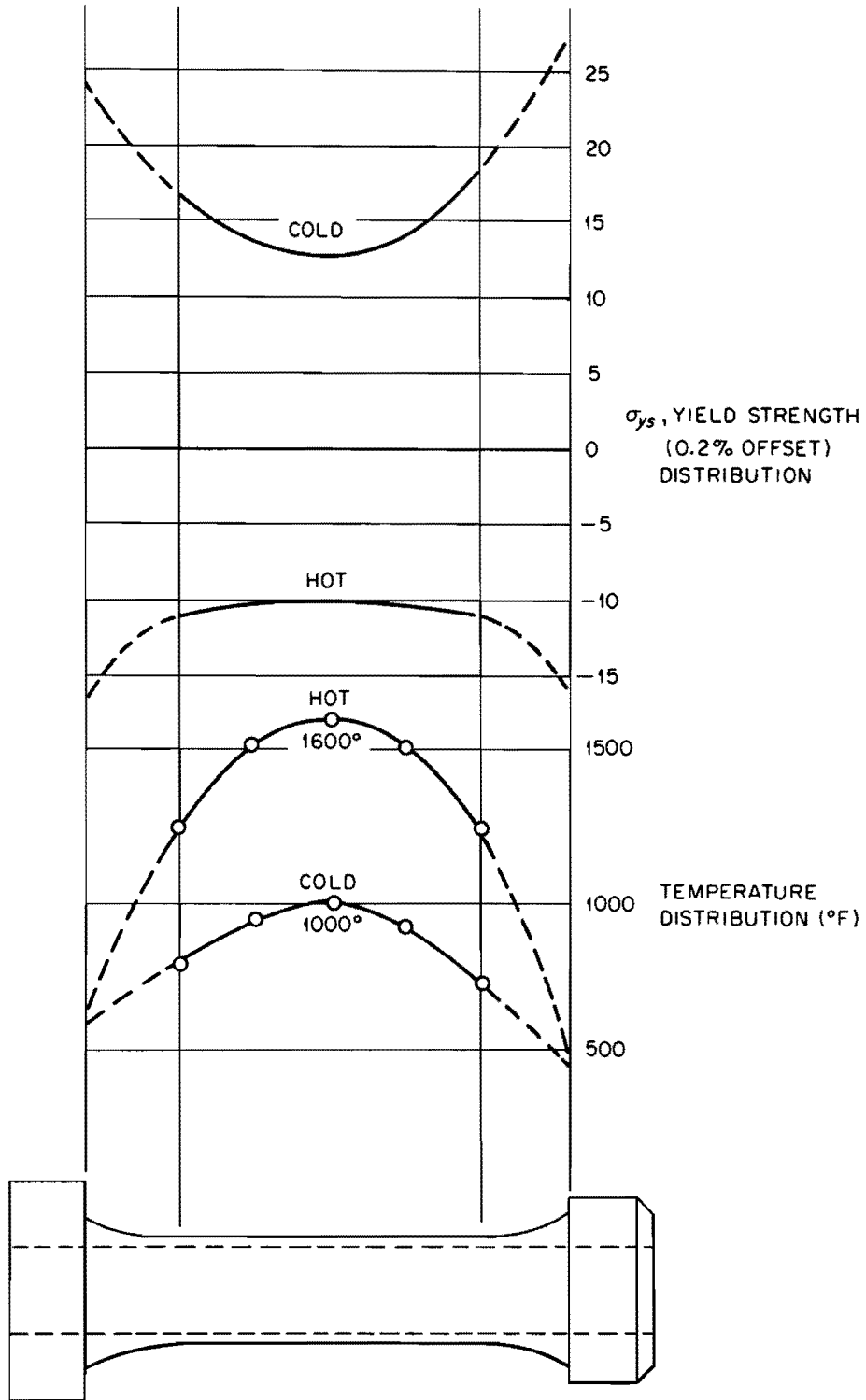


Fig. 5. Temperature and Yield Strength Distribution.

For the actual case $(\Delta T)_x$ is not uniform throughout the length. The effective length L° is related to ΔT at midlength by

$$L^\circ = \frac{\Delta D^\circ}{\alpha (\Delta T)_{\text{mid}}} . \quad (34)$$

The length L° represents $(L_1 + L_2)$ of the simplified case. The value of L° is always greater than the length of the straight section and is nearly equal to the distance between the massive ends of the specimen. It is absolutely necessary that the model specimen be composed of two distinct lengths and areas because in a real specimen (1) the fillets are larger in area and constitute about one third of the total length, (2) the fillets cycle in temperature and contribute to the δ_T , and (3) the fillets sustain little, if any, plastic strain.

The width of the load-temperature loop at zero load is $(T_b - T_e)$. The length $(L_1 + L_2)$ is simply L° as described above. The length L_2 of the model is the length sustaining a uniform distribution of plastic strain. In the actual case the unit plastic strain is not uniformly distributed; however, the total plastic strain is

$$\Delta \epsilon_p = \alpha (T_b - T_e) L^\circ . \quad (35)$$

This method of determining the total plastic strain can be used and a secondary strain-measuring system employed to determine the average unit plastic-strain value of the center 1 in. of the specimen length. An effective gage length L' defines the relationship of the total plastic strain of Eq. (35) to the average $\Delta \epsilon_p$ value determined by the secondary measuring system.

$$L' = \frac{\Delta \epsilon_p}{\Delta \epsilon_{p_{\text{av}}}} . \quad (36)$$

The value of L' represents L_2 of the simplified case and is defined as the ratio of the total plastic strain of the specimen to the average unit plastic strain of a short central length of the specimen. The temperature is almost uniform in this length, and a posttest examination of the specimen will indicate if the plastic strains were nearly uniform.

To obtain the average $\Delta\epsilon_p$ of a central length a sensitive strain measuring system, preferably an optical one, is used to measure the total geometric displacement δ_c of markers placed at the ends of this length. During the temperature cycle the displacement δ_c is the thermal strain plus the mechanical strain.

$$\delta_c = \delta_T + \delta_m \quad . \quad (37)$$

Because the gage length is unity,

$$\Delta\delta_c = \alpha\Delta T + \frac{\Delta\sigma}{E} + \Delta\epsilon_{p_{av}} \quad . \quad (38)$$

If two points of the P-T cycle are conveniently chosen at the zero load condition on heating and cooling, the elastic component of Eq. (38) is zero, and

$$\Delta\epsilon_{p_{av}} = -\alpha (T_b - T_e) + \Delta\delta_c \Big|_b^e \quad . \quad (39)$$

The effective gage length L' for the test is

$$L' = \frac{\alpha (T_b - T_e) L^\circ}{-\alpha (T_b - T_e) + \Delta\delta_c \Big|_b^e} \quad . \quad (40)$$

That L' and L° are not equal ought to be obvious. The length L' is not a constant for all tests. It is dependent on the maximum temperature, the temperature difference, the material, and the specimen geometry. To determine L' for one test and apply it to all test conditions will produce an erroneous slope to the $\log \Delta\epsilon_p$ vs $\log N_f$ curve.

A very simple method for approximating L' can be employed without special strain-measuring devices. On specimens sustaining large values of cyclic plastic strain, the machined surface of the straight section is disturbed by the deformation. The length of this deformed region can be easily measured after the test and is approximately equal to L' . For very small values of plastic strain, the specimen surface is undisturbed and L' is nearly equal to the straight portion of the sample.

The value of L' decreases with increasing values of $\Delta\epsilon_p$ and maximum temperature. Demers⁹ has shown the value of L' to be stable during the test period and to increase slightly for increasing wall thickness. For the wall thicknesses investigated (0.020 to 0.060 in.), only a slight change of the temperature profile was noted. The effect of using values of both L' and L° in error in the order of 0.25 in. will produce an error of about 25% in the computed strain value.

The tubular specimen design is susceptible to geometric instabilities that make it unsuitable as a standard, or reference, test specimen. Tubular specimen data are conservative, however, and this is not without merit. However, the influence of the specimen geometry must be considered if thermal-fatigue data are to be appreciated.

Method I, Eq. (10). - The plastic-strain range by Method I is

$$\Delta\epsilon_p = \alpha (\Delta T)_o \frac{L^\circ}{L'} \quad (41)$$

where $(\Delta T)_o$ is the width of the load-temperature loop at zero load. Because $L^\circ = \frac{\Delta D^\circ}{\alpha \Delta T_{\max}}$, it is not necessary to state the value of α

explicitly. Equation (41) can be rewritten

$$\Delta\epsilon_p = \frac{(\Delta T)_o \Delta D^\circ}{(\Delta T)_{\max} L'} \quad (42)$$

Two of the objections to the thermal-fatigue test are that the modulus of elasticity, the thermal coefficient, and the strength of the material vary with temperature and that the thermal coefficient varies with stress. Thus, say the critics, a large uncertainty is included in any calculated value of $\Delta\epsilon_p$. To determine $\Delta\epsilon_p$ by Eq. (42), the values of E , α , and the calibration factor of the load cell are not required. It is trivial to show that α is stress dependent for the plastic strain as calculated by measuring the width of the P-T loop at two zero stress conditions.

⁹G. Z. Demers, Effect of Varying the Wall Thickness of Tubular Specimens in Thermal-Strain Cycling of 304 Stainless Steel, M. S. Thesis, University of Alabama (January 1962).

An analogy of Eq. (42) can be described in three steps. First, the length of an unloaded bar is measured. Second, the bar is heated (or cooled) in a restrained condition and sustains plastic flow. Third, the bar is unloaded and the length remeasured. Equation (42) provides a means for calculating the amount of plastic flow that results from constrained thermal loading without regard to the variation of properties during that period.

The temperatures of zero load on heating and cooling are near the mean temperature of the test; therefore, if α is used to determine L' , α at the mean temperature is the better choice. Thus, the assumption of α and E being independent of stress and temperature is seen to be reasonable.

Method II, Eq. (13). - Equation (13) can be rewritten to allow calculation of $\Delta\epsilon_p$ by

$$\Delta\epsilon_p = \alpha (\Delta T)_{\max} \frac{L^\circ}{L'} - \frac{\Delta\sigma_1}{E} \left(\frac{L_1}{L'} \right) - \frac{\Delta\sigma_2}{E} - \frac{\Delta P}{K_s L'} \quad (43)$$

The necessity of evaluating ΔP , E , L_1 , A_1 , and K_s adds additional uncertainties that are not included in Method I. The value L_1 can be approximated by $(L^\circ - L')$. The omission of $\frac{L^\circ}{L'}$ will produce an error in the slope of the $\log \Delta\epsilon_p - \log N_f$ curve. Because many materials relax at elevated temperature, the relaxed or final values of stress and load at the maximum and minimum temperatures must be used if Eq. (43) is to be correctly used. The approximation of Eq. (43) by

$$\Delta\epsilon_p = \alpha (\Delta T)_{\max} - \frac{\Delta\sigma_2}{E} \quad (44)$$

is unnecessarily conservative (i.e., it gives too low a value of $\Delta\epsilon_p$).

Method III, Eq. (18). - This equation can be applied to the actual case by

$$\Delta\epsilon_p = - \frac{P_f - P_c}{L'} \left(\frac{L^\circ - L'}{A_1 E} + \frac{1}{A_2 E} + \frac{1}{K_s} \right) \quad (45)$$

The evaluation of an effective area A_1 is inconvenient, and a constant temperature line must be selected that intersects the linear portion of the heating and cooling curves. Equation (45) will be applicable

only to high-strength, low-ductility materials. To neglect the deflection of the restraint and reduce Eq. (45) to

$$\Delta\epsilon_p = -\frac{\Delta\sigma_2}{E} \Big|_c^f \quad (46)$$

is unjustified. A calculation of $\Delta\epsilon_p$ by Eq. (46) will generally lead to errors of 100% or greater. Two points on an isothermal line of the load-temperature loop do not have equal strain values in the stress-strain graph as indicated in Fig. 3.

Discussion of Geometric Stability

A graph of the actual temperature profiles of a test having a temperature cycle at midlength of 1000 to 1600°F is shown in Fig. 5. The yield strength at 0.2% offset is also shown as a function of temperature, and the stresses required to produce a plastic strain of 0.2% at the maximum and minimum temperature profile values are shown as a function of the length of the sample. At 1600°F almost no strain hardening exists, but at 1000°F some will be observed. It is concluded that the plastic-strain distribution at the maximum temperature is not equal to the distribution at the minimum temperature. The lack of equality of the local plastic strain on heating and cooling means that the compressive plastic strain is not equal to the tensile plastic strain. Thus, the plastic Poisson strains (in the radial and circumferential directions) should be cumulative. Near the center of the specimen this accumulation is positive and the diameter and wall thickness seem to "grow" during continued cycling. After a growth of the circumference, the test specimen is no longer a right circular cylinder and longitudinal instabilities may cause the specimen to buckle.

An increase in wall thickness in the central length and a decrease near the specimen ends are also effects of the growth process. The electrical resistance per unit length is maximum in the thin region and minimum in the thick region. For resistance heating, a larger release of heat occurs near the specimen ends and the temperature distribution is changed considerably. Thus, the resistance-heating

method of the conventional test can have a significant effect on the results. The probability of this process reversing itself to cause growth in the thin section and depletion of material in the center is almost nil. One reason why thermal-fatigue and isothermal strain-fatigue data do not always show good agreement may be related to the instability of specimen geometry and the compounding of this phenomenon by the heating method.

Thomas¹⁰ has reported in detail the dimensional changes of resistively heated specimens. Sims¹¹ obtained a time lapse motion picture of the phenomena of bulging and temperature profile change, and these have been reported elsewhere.¹² Demers demonstrated that the tendency for growth and buckling was minimized by using a larger wall thickness.⁹

For type 304 stainless steel, $\Delta\epsilon_p$ and N_f values from thermal-fatigue and isothermal strain-fatigue tests (Fig. 6) are equal at large values of N_f . Here, no measurable geometric (or temperature profile) changes occur in the thermal-fatigue test, and the failure is only the formation and propagation of a fatigue crack. A typical sample is shown in Fig. 7. In the region where isothermal and thermal-fatigue data show considerable disagreement, i.e., at large values of $\Delta\epsilon_p$ and low N_f , geometric modifications always occur similar to that shown in Fig. 8.

¹⁰W. S. Thomas, An Investigation of the Stages of Deformation of a Thin-Wall Tube Caused by Cyclic Thermal Stress, M. S. Thesis, University of Alabama (August 1961).

¹¹J. D. Sims, "Prediction of Cycles to Failure for Thermally Stressed Stainless Steel," paper presented at the 1961 Southeastern Regional Student Conference of the IAS (May 1961).

¹²A. E. Carden and J. H. Sodergren, "The Failure of 304 Stainless Steel by Thermal-Strain Cycling at Elevated Temperature," paper presented at the ASME Annual Meeting, November 26-December 1, 1961, New York, 61-WA-200 (1961).

UNCLASSIFIED
ORNL-LR-DWG 71555

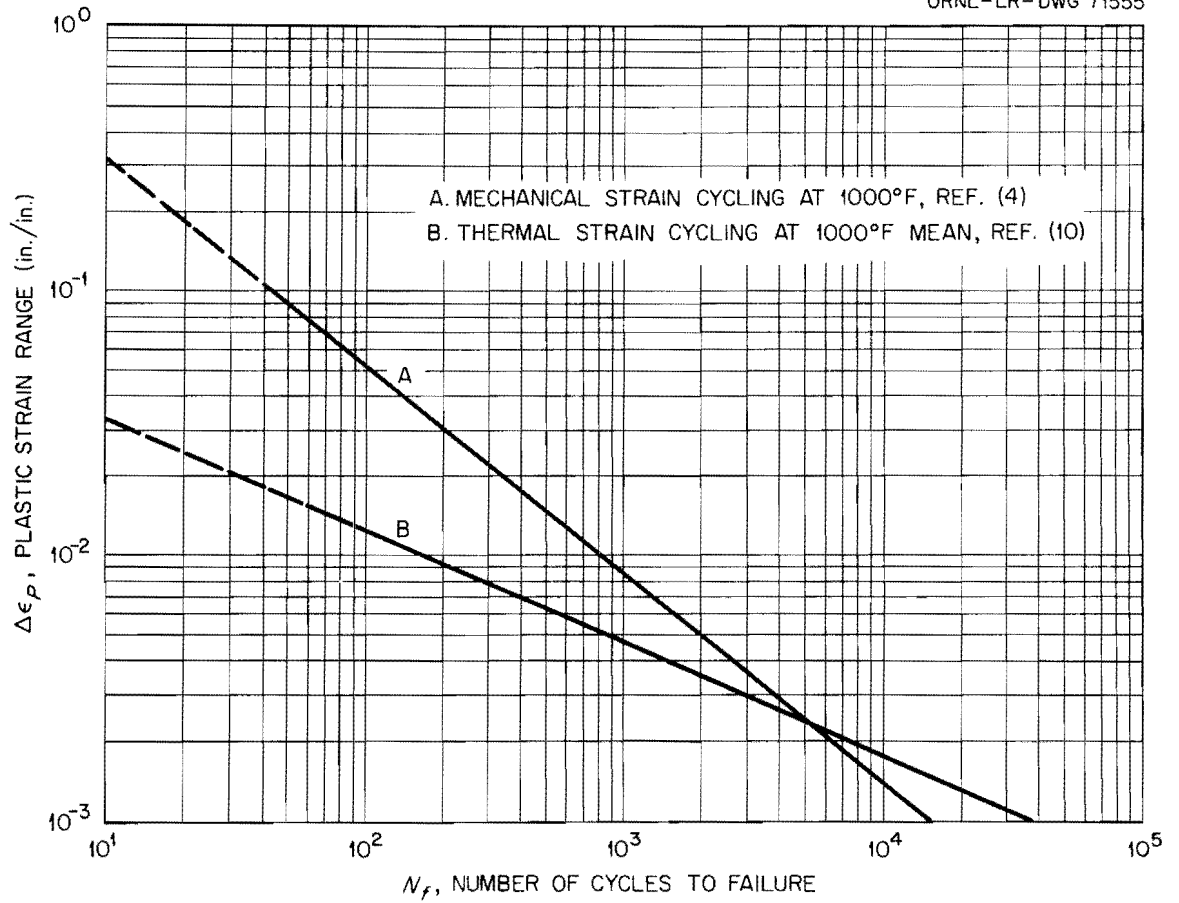
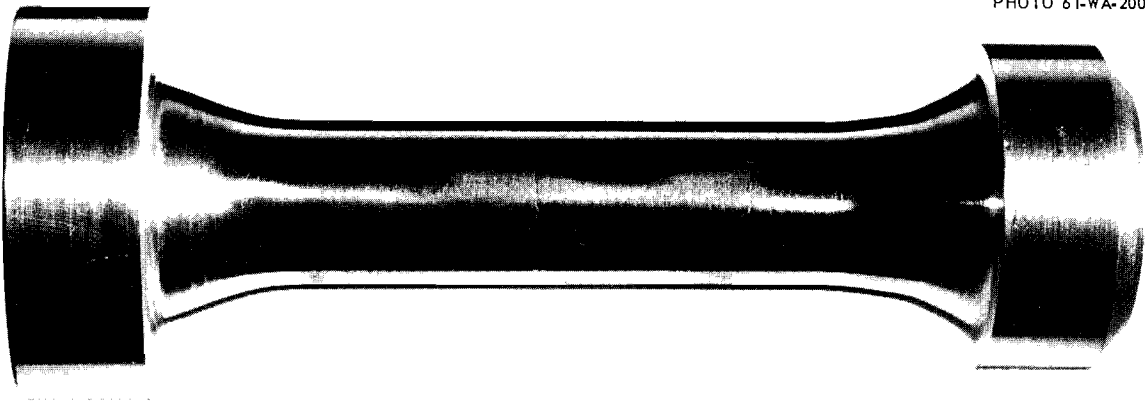


Fig. 6. Comparison of Thermal- and Isothermal-Fatigue Results.

UNCLASSIFIED
PHOTO 61-WA-200



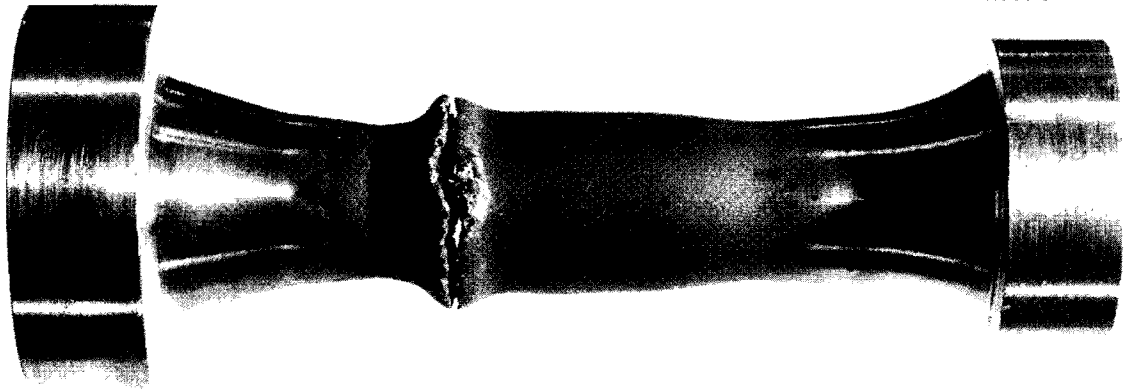
S II-11

Mean Temperature: 900°F; Limits: 700-1100°F

N_f : 121,868; ϵ_p : 912 $\mu\text{in./in.}$

Fig. 7. Specimen Appearance at Large Number of Cycles to Failure.

UNCLASSIFIED
PHOTO 61-WA-200



S II-4

Mean Temperature: 1100°F; Limits: 700-1500°F

N_f : 277; ϵ_p : 8600 $\mu\text{in./in.}$

Fig. 8. Specimen Appearance at Small Number of Cycles to Failure.

Constancy of Parameters

The values of $\Delta\epsilon_p$ and $\Delta\sigma$ will not be constant during the test if strain hardening or strain softening occurs. The variations of $\Delta\sigma$ during the life of two tests are shown in Fig. 9. When reporting data, the parameter should be defined as the initial value (first half cycle), average value (average of all cycles), or asymptotic value (variation extrapolated to the last cycle). Manson¹³ has demonstrated that the asymptotic value is preferred.

Temperature Profiles

To obtain the temperature profiles for thermal cycling, five thermocouples are spot welded to the specimen, one at the center of the gage length and one at each 1/2-in. interval above and below the center. The output of a potentiometer and the five thermocouples are attached to the input of a thermocouple switch. The output of the switch is attached to a direct-current millivolt recorder. As the specimen is thermally cycled, the output of each thermocouple is switched to the recorder for several cycles, and the thermocouple electromotive force is recorded as a function of time. The potentiometer is then set on certain values of electromotive force and is connected to the recorder input to provide calibration to the chart. The arrangement is shown schematically in Fig. 10.

Actual P-T Loop

The accuracy of the actual load-temperature hysteresis loop can be improved by connecting the five thermocouples in parallel and plotting the average electromotive force vs load. The actual value of L° is thus obtained and compensation is provided for any change that may occur in the area between the temperature profiles during the test period. The probability of thermocouple failure is, of course, increased fivefold by this arrangement.

A strong statement is presented favoring the use of the load-temperature loop. Much information can be gleaned from these diagrams, from which the behavior of the material is easily ascertained. Many

¹³S. S. Manson, Seminar on "Materials Under Thermal Stress," Pennsylvania State University (August 1961).

UNCLASSIFIED
ORNL-LR-DWG 71556

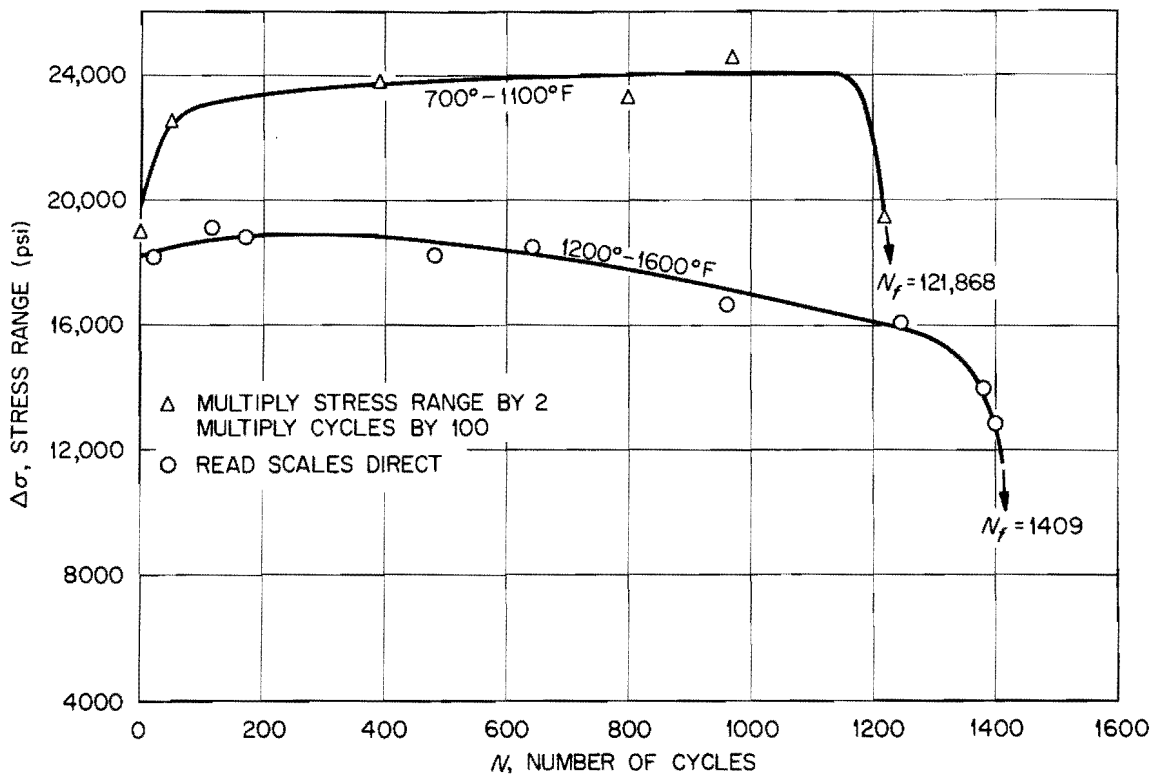


Fig. 9. Variation of Stress Range During Thermal-Fatigue Test.

UNCLASSIFIED
ORNL-LR-DWG 71557

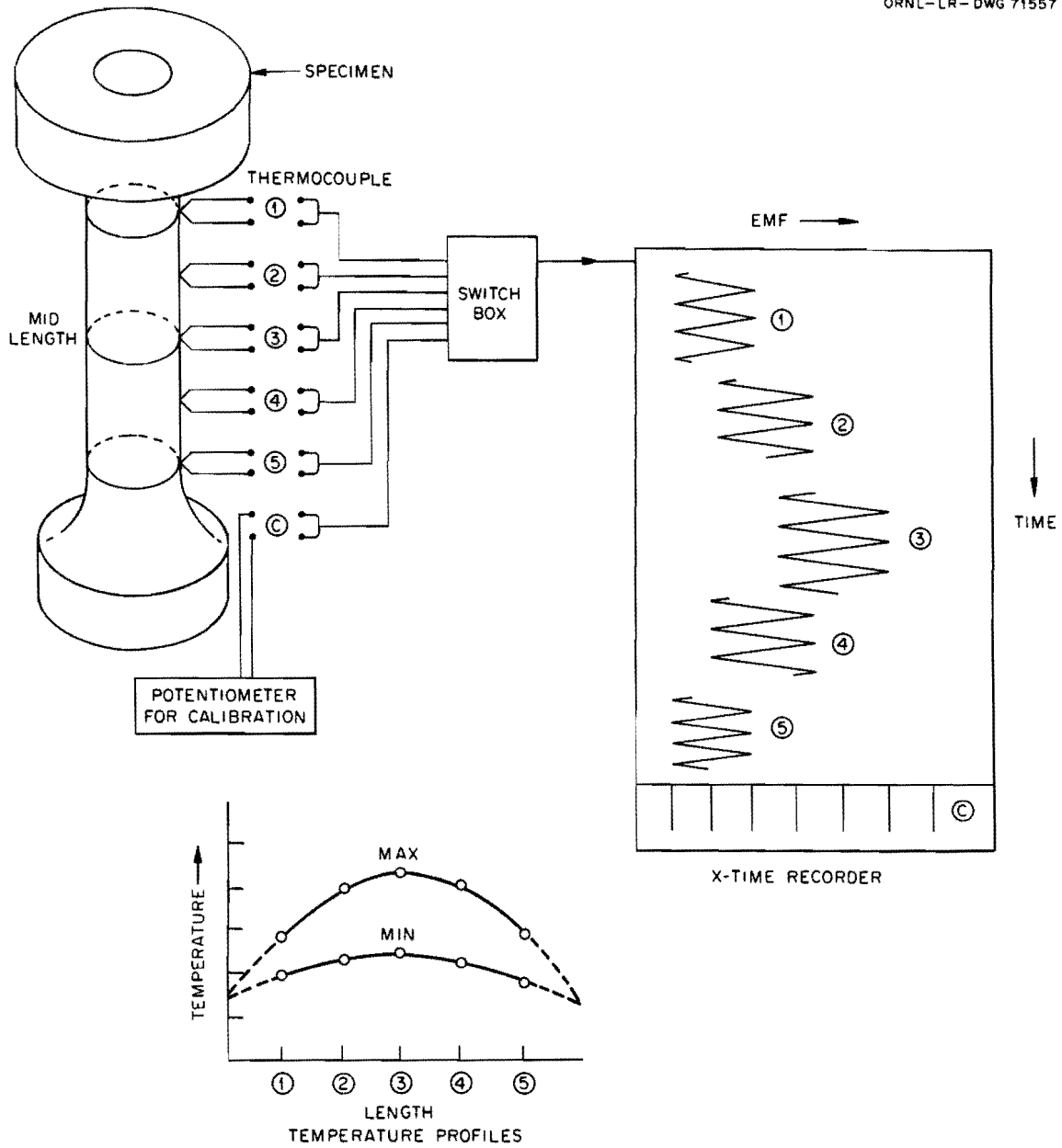


Fig. 10. Schematic of Method of Obtaining Temperature Profiles.

x-y recorders will accept direct-current millivolt inputs without additional instrumentation. The load cell output, suitably amplified, is used to drive the y axis; the thermocouple output supplies the x axis signal. Thus an autographic P-T cycle is readily obtained.

The P-T loop shown in Fig. 11a indicates the decrease of elastic strength near the maximum temperature. The relaxation of elastic stress that occurs during the hold time at the maximum temperature is shown in Fig. 11b. Slack in the clamping mechanism is apparent in the loop of Fig. 11c and elastic cycling is shown in Fig. 11d. Strain hardening and strain softening can be easily detected, and the area of the P-T cycle is proportional to the plastic-strain energy dissipated per cycle. The plastic-strain energy, the plastic-strain range, the mechanical-strain range, and the stress range can all be determined from the P-T loop. These variables as related to the P-T loop are summarized in Appendix C. Neglecting geometric effects, if the stress-temperature and temperature-time paths of two tests are identical, the results should be equal.

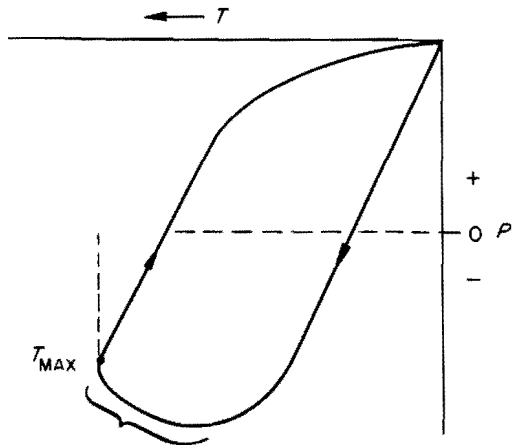
The Stress-Strain Diagram

A stress-strain hysteresis loop can be plotted if data are obtained from the load cell, temperature at midlength of the specimen, and a dial gage that measures the displacement of the restraint. A typical data sheet is shown in Fig. 12. The temperature cycle is divided into convenient increments; and, at these temperatures, readings are obtained from the load cell and dial gage. The stress change over the increment is

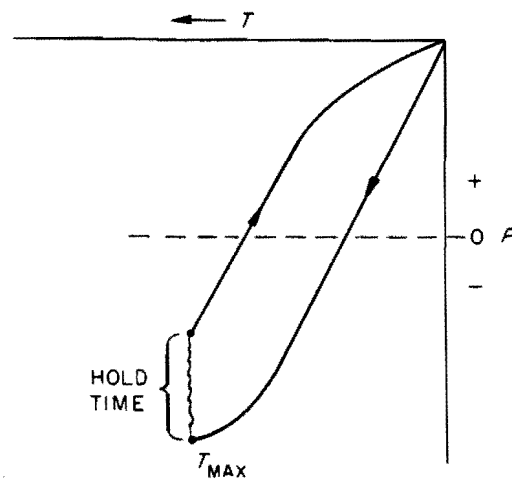
$$\Delta\sigma = \frac{(\Delta SR-4)(C.F.)}{A_2} \quad (47)$$

The change in load-cell output is $\Delta SR-4$, (C.F.) is the calibration constant of the load cell in pounds per microunit, and A_2 is the minimum cross-sectional area (the area of the gage portion) of the specimen.

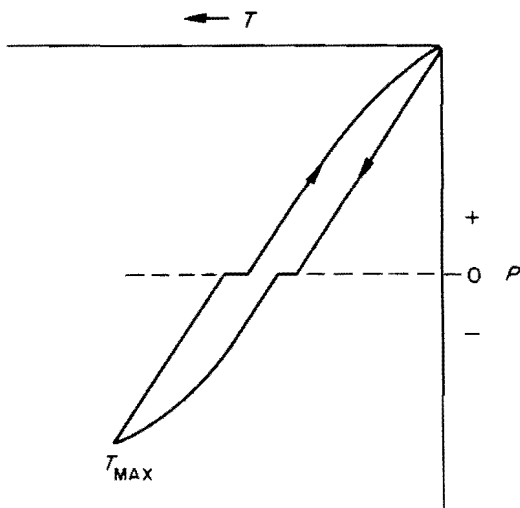
Over the same interval of temperature the unit mechanical-strain change is calculated from the temperature increment ΔT and the increment of dial gage change $\Delta D'$.



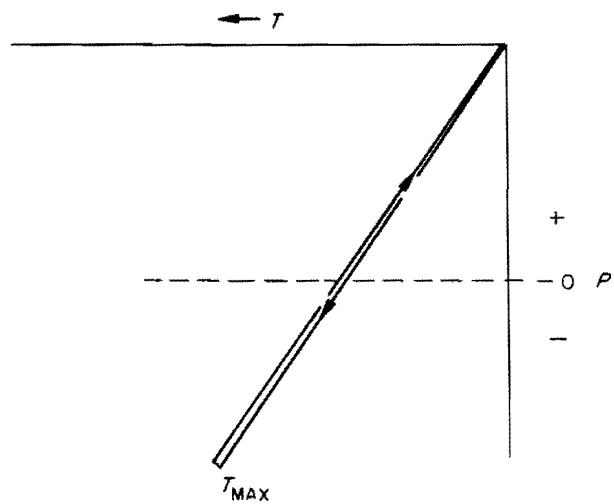
(a) DECREASE IN ELASTIC STRENGTH
DURING LATER PORTION OF
HEATING PERIOD



(b) RELAXATION DURING HOLD TIME



(c) SLACK IN CLAMPING MECHANISM



(d) ELASTIC CYCLING

Fig. 11. Typical P-T Loops.

Temperature Limits: 850 to 1550°F; Cycle No. 20 to 24; $\Delta\epsilon_p = 0.009210$;

Area of Specimen: 0.03789 in.²; $\alpha = 11.65 \times 10^{-6}$; $L^o = 2.43$ in.;

$L' = 1.58$ in.; Dial Gage Difference (free): 0.01983 in; $N_f = 62$

Temp (°F)	SR-4 Range	Reading μin./in.	Δ SR-4 μin./in.	$\Delta\sigma$ psi	$\Delta\epsilon_m$ μin./in.	$\alpha\Delta T \frac{L^o}{L'}$ μin./in.	$\frac{\Delta\bar{D}}{L'}$ μin./in.	$\Delta\bar{D}$ in.	\bar{D} Dial Gage 10^{-4} in.
850	0-18	80		0	0	0	0		83
	0-18		220					0.0006	
950	0-18	300		24,210	1411	1790	379		89
	0-18		380					0.0012	
1050	0-18	460		41,820	2822	3580	758		95
	0-18		460					0.0015	
1150	0-18	540		50,625	4422	5370	948		98
	0-18		500					0.0016	
1250	0-18	580		55,030	6149	7160	1011		99
	0-18		500					0.0016	
1350	0-18	580		55,030	7939	8950	1011		99
	0-18		470					0.0016	
1450	0-18	550		51,730	9729	10,740	1011		99
	0-18		400					0.0014	
1550	0-18	480		44,020	11,646	12,530	884		97
	0-18		400					0.0014	
1450	0-18	270		20,910	10,235	10,740	505		91
	0-18		190					0.0008	
1350	0-18	190		11,000	8634	8950	316		88
	0-18		110					0.0005	
1250	0-18	150		7700	6907	7160	253		87
	0-18		70					0.0004	
1150	0-18	130		5500	5180	5370	190		86
	0-18		50					0.0003	
1050	0-18	110		3300	3454	3580	126		85
	0-18		30					0.0002	
950	0-18	90		1100	1727	1790	63		84
	0-18		10					0.0001	
850	0-18	80		0	0	0	0		83

Fig. 12. Data Sheet for Thermal-Fatigue Stress-Strain Diagram - Type 304 Stainless Steel.

$$\Delta\epsilon_m = \alpha\Delta T \frac{L^o}{L'} - \frac{\Delta D'}{L'} \quad (48)$$

The data of columns 1, 2, 3, and 10 are used to calculate the stress and strain values of columns 5 and 6 of Fig. 12. If one assumes an arbitrary zero of the coordinate system to be at the minimum temperature, all of the loop will appear in the third quadrant. The data of Fig. 12 were used to plot the hysteresis loop of Fig. 13. The slope of the σ - ϵ diagram at zero load is about 19×10^6 psi, which shows rather good agreement to the modulus of elasticity value at 1200°F.

A stress-temperature loop constructed from the data is shown in Fig. 14, and a 515°F maximum width is observed. The $\Delta\epsilon_p$ values evaluated from several methods are

σ-ε loop	0.009210	}	Average 0.008824
Method I	0.008620		
Method II	0.008594		
Equation (44)	0.005410		

Method III is applicable only in tests of materials having large values of elastic strength. It is not used for this example because of the lack of sufficient elasticity. Because Eq. (44) is so widely used, the results obtained from it are included to illustrate the disparity of values. For small values of $\Delta\epsilon_p$, Eq. (44) yields much smaller values than Method I or II. There have been occasions reported where Eq. (44) was used and a negative $\Delta\epsilon_p$ value was obtained.¹⁴ This is easily explained. The value $\Delta\epsilon_p$ may be approximated by $\alpha\Delta T (F) - \frac{\Delta\sigma}{E}$. The constraint factor F is greater than 1 and for the example cited is 1.43. For a material with sizeable elastic strength and a test producing little or no $\Delta\epsilon_p$, it is obvious that $\frac{\Delta\sigma}{E}$ could be larger than $\alpha\Delta T$; if the constraint factor is neglected, the calculated value of $\Delta\epsilon_p$ is negative.

An autographic stress-strain loop is obtained if the difference of the outputs of a displacement transducer and the output of a temperature transducer is used to drive the strain axis. During free

¹⁴K. E. Horton and R. S. Stewart, Final Report. Thermal-Stress-Fatigue Behavior of Zirconium and Zirconium Alloys, ATL-A-127 (October 31, 1961).

UNCLASSIFIED
ORNL-LR-DWG 71559

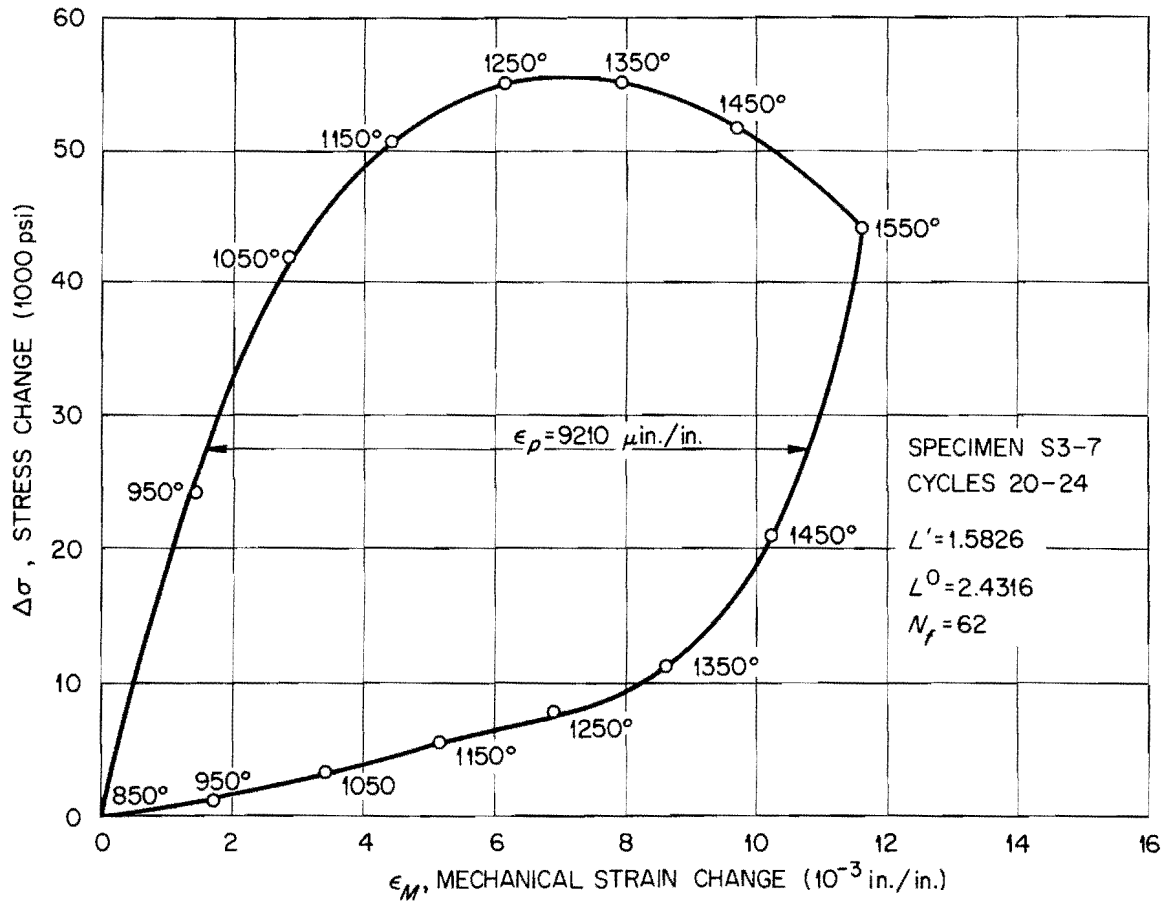


Fig. 13. Thermal-Fatigue Stress-Strain Diagram.

UNCLASSIFIED
ORNL-LR-DWG 71560

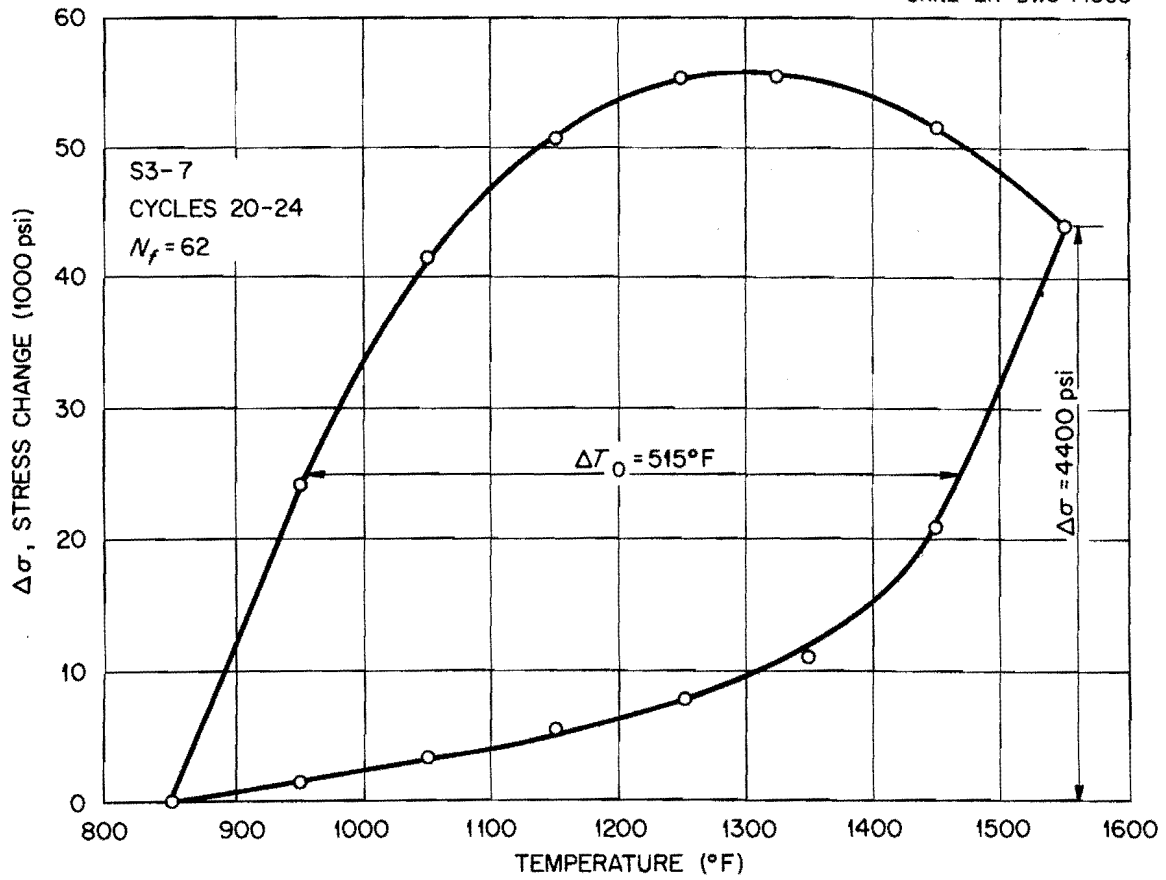


Fig. 14. Thermal-Fatigue Load-Temperature Loop.

cycling the outputs of the temperature and dial gage transducers are made to be equal and opposite. In essence, the mechanical strain δ_m of Eq. (5) is being plotted vs load. A scale factor for each axis must be determined.

ALTERNATE TEST METHODS

Segmented-Type Tubular Test Specimen

A significant modification of the conventional test method has been reported by Wylie, Hoggatt, and Venuti.¹⁵ A hollow segmented-type specimen and induction heating were used with considerable improvement of the temperature profile. The reduced diameter of the test specimen is located at a greater distance from the induction coil. The heating rate decreases rapidly as the spacing increases; therefore, the ends of the gage length receive much larger amounts of power during heating. The longitudinal temperature distribution is nearly uniform. The effective length L' is equal to the central length of the specimen. Radial temperature distributions for induction heating become significant for thick sections or rapid heating rates. For the tests reported this did not seem to manifest any unique difficulties. Although growth of the specimen diameters was observed, the data are consistent and in agreement with the low-cycle-fatigue equation

$$\Delta \epsilon_p N_f^a = -1/2 \ln \left(\frac{100 - ROA}{100} \right).$$

For tubular specimen geometries the specimen design suggested by Wylie, Hoggatt, and Venuti and induction heating offer several advantages: (1) the longitudinal temperature profile is greatly improved, (2) the effective gage length L' is determined without the use of special strain-measuring devices, and (3) various degrees of constraint can be obtained by varying the length of the reduced section or by changing the number of windings of the induction coil.

Servocontrolled Testing Machines

Testing machines are currently available that are capable of accurately controlling the heating rate and stress rate according to

¹⁵E. B. Wylie, C. Hoggatt, and R. Venuti, The Effects of Thermal Cycling Between Cryogenic and Elevated Temperatures on the Mechanical Properties of Materials, DRI-1576-FR, University of Denver (March 15, 1961).

a preselected program. Both parameters are separately, although synchronously, controlled. Thus, almost any stress-temperature-time cycle can be obtained in a test.

An Alternate Thermal-Fatigue Test

Many axial-stress-fatigue tests employ "zero gage length" solid test specimens. The employment of such a specimen design as shown in Fig. 15 in thermal fatigue would be of vital benefit in improving the geometric stability. A uniform longitudinal temperature distribution is not required; it is only necessary that the maximum temperature occurs in the minimum cross section. Simultaneous use of induction and resistance heating will produce a uniform radial temperature. Only the diametral strain and temperature need to be recorded as functions of load in order to compute the actual plastic-strain range in the minimum cross section.

To determine the plastic-strain range, a load-temperature and a load-diametral strain loop are obtained, as shown in Fig. 16. The geometric strain in the Z direction ϵ_{gz} is defined as the strain which is measured directly; this geometric deformation is the sum of the thermal and mechanical strains.

$$\epsilon_{gz} = \epsilon_{Tz} + \epsilon_{mz} , \quad (49)$$

or

$$\epsilon_{gz} = \alpha T + \frac{\sigma_z}{E} + \epsilon_{pz} . \quad (50)$$

For a uniaxial load in the Z direction, the geometric strain in the radial direction is

$$\epsilon_{gr} = \epsilon_T + \epsilon_{mr} , \quad (51)$$

or

$$\epsilon_{gr} = \alpha T - \mu \left(\frac{\sigma_z}{E} \right) - 1/2 (\epsilon_{pz}) . \quad (52)$$

The radial geometric strain can be obtained from a transducer arrangement like that shown in Fig. 17. The radial geometric strain for a minimum radius of R is

$$\epsilon_{gr} = \frac{\Delta D}{2R} , \quad (53)$$

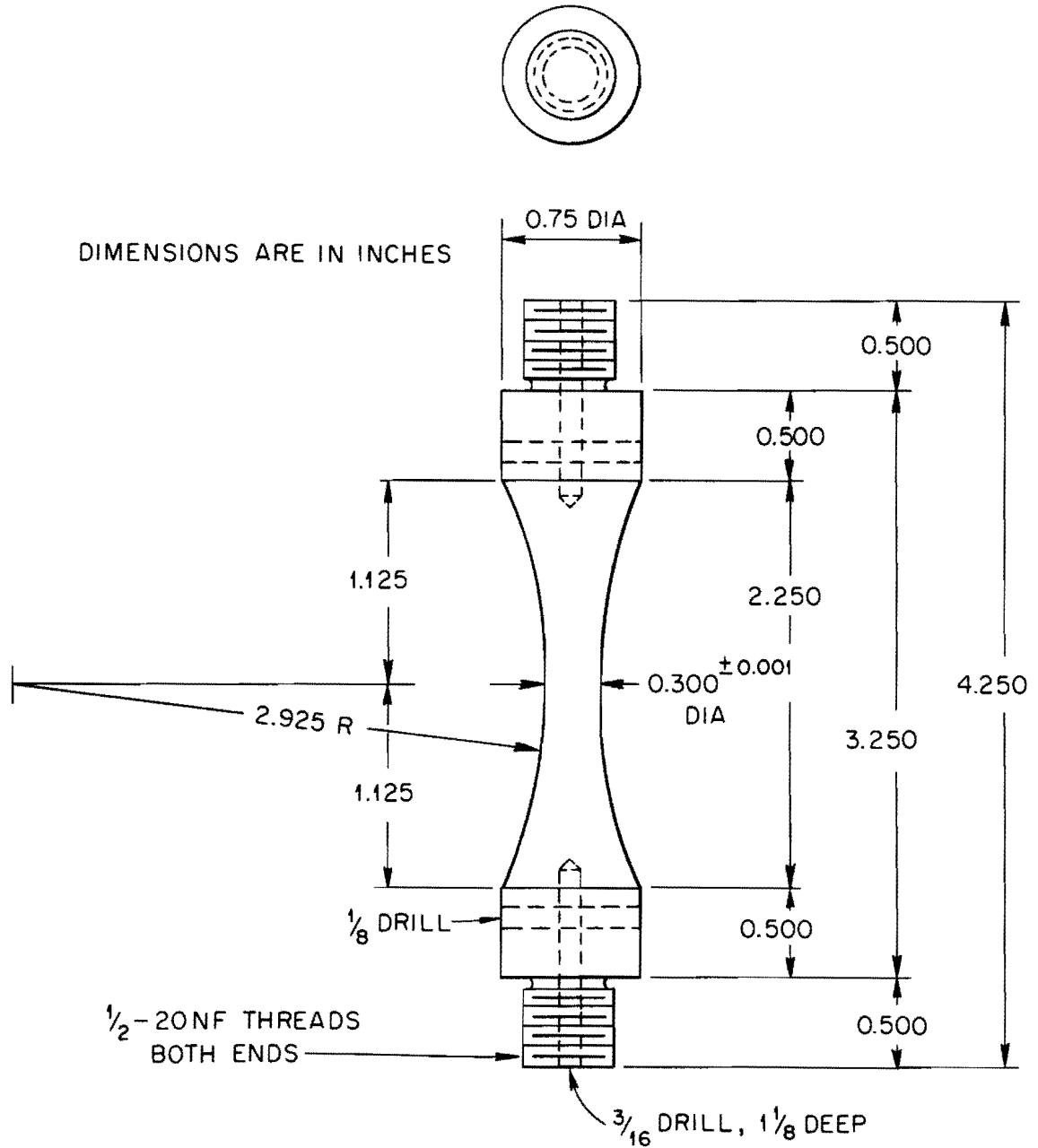
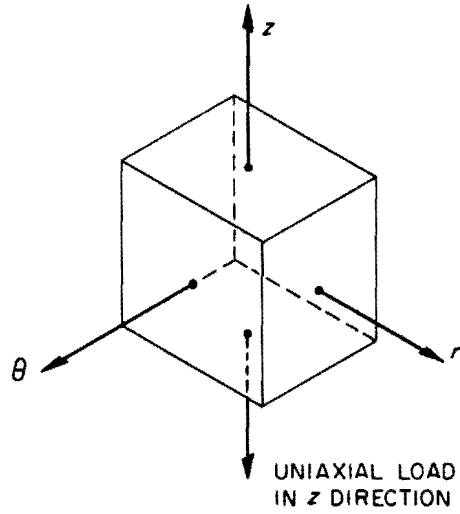
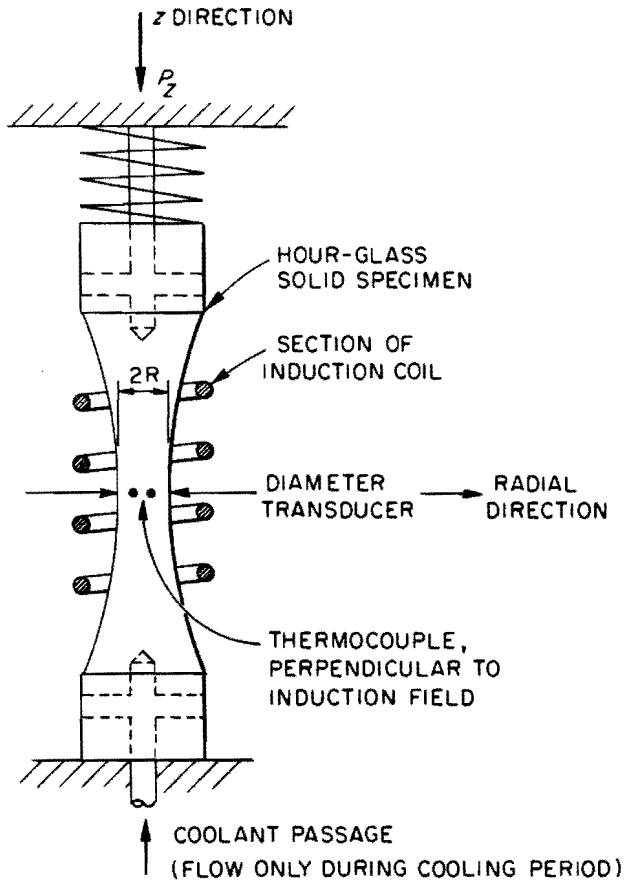


Fig. 15. Thermal-Fatigue Solid Test Specimen.

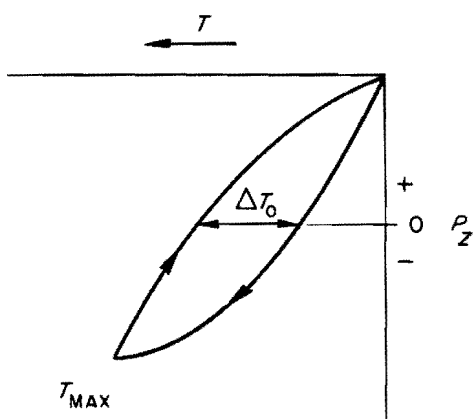
UNCLASSIFIED
ORNL-LR-DWG 71562



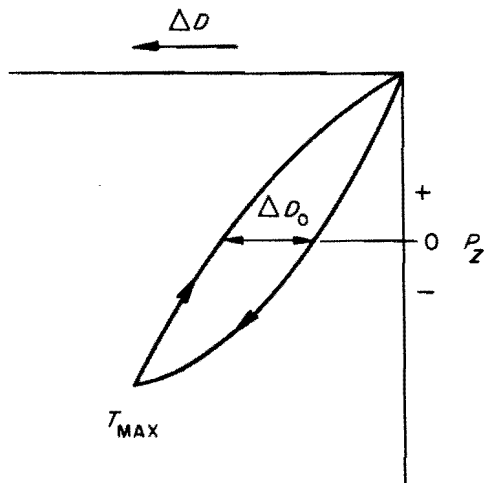
$$\epsilon_{gz} = \alpha T + \frac{\sigma_z}{E} + \epsilon_{pz}$$

$$\epsilon_{gr} = \alpha T - \nu \frac{\sigma_z}{E} - \frac{\epsilon_{pz}}{2}$$

$$\epsilon_{gr} = \frac{\Delta D}{2R}$$



P-T LOOP



P- ΔD LOOP

Fig. 16. Alternate Thermal-Fatigue Test.

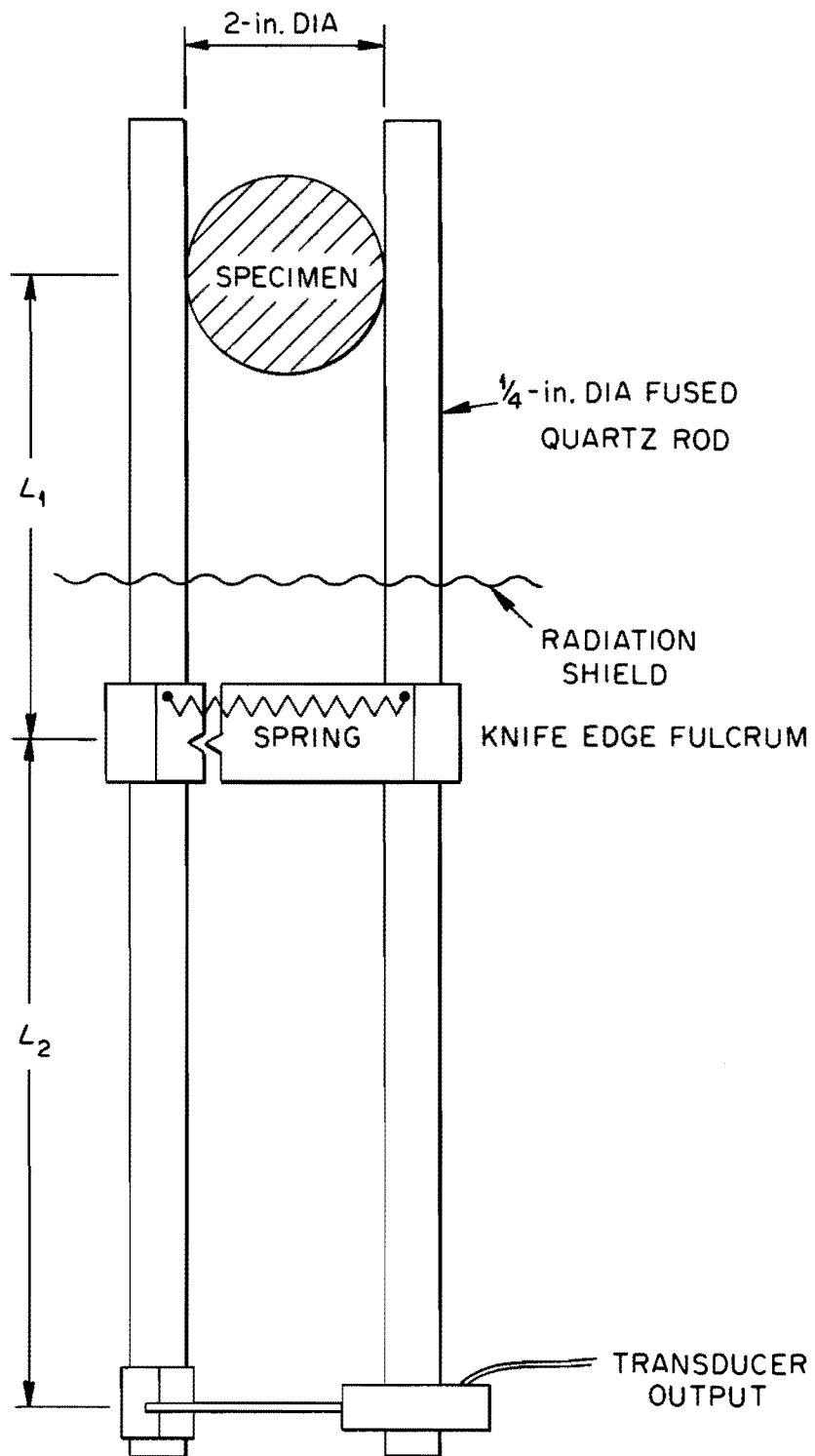


Fig. 17. Diametral Strain Gage.

or

$$\frac{\Delta D}{2R} = \alpha \Delta T - \mu \left(\frac{\Delta \sigma_z}{E} \right) - \frac{\Delta \epsilon_{pz}}{2} \quad (54)$$

The plastic-strain range can be conveniently calculated by measuring ΔT and ΔD at the zero load condition. The elastic-strain term is zero and

$$\Delta \epsilon_{pz} = 2 \left[\alpha (\Delta T)_0 - \frac{(\Delta D)_0}{2R} \right] \quad (55)$$

The mechanical-strain range in the radial direction is

$$- \epsilon_{mr} = \alpha (\Delta T)_{\max} - \frac{(\Delta D)_{\max}}{2R} \quad (56)$$

The mechanical-strain range in the radial direction is

$$\Delta \epsilon_{mr} = - \mu \Delta \epsilon_{ez} - 1/2 \Delta \epsilon_{pz} \quad (57)$$

Substituting Eq. (57) into (56),

$$\mu \Delta \epsilon_{ez} + 1/2 \Delta \epsilon_{pz} = \alpha \Delta T - \frac{\Delta D}{2R} \quad (58)$$

or

$$2\mu \frac{\Delta \sigma_z}{E} + \Delta \epsilon_{pz} = 2\alpha \Delta T - \frac{\Delta D}{R} \quad (59)$$

Subtracting $(2\mu - 1) \frac{\Delta \sigma_z}{E}$ from both sides

$$\frac{\Delta \sigma_z}{E} + \Delta \epsilon_{pz} = 2\alpha \Delta T - \left[\frac{\Delta D}{R} + (2\mu - 1) \frac{\Delta \sigma_z}{E} \right] \quad (60)$$

The mechanical-strain range in the Z direction is therefore

$$\Delta \epsilon_{mz} = 2\alpha \Delta T - \left[\frac{\Delta D}{R} + (2\mu - 1) \frac{\sigma_z}{E} \right] \quad (61)$$

The unit plastic-strain energy per cycle is equal to $\frac{2\alpha}{A}$ times the area of the P-T loop minus $\frac{1}{AR}$ times the area of the P - ΔD .loop.

$$W_p = \frac{2\alpha}{A} \int P (dT) - \frac{1}{AR} \int P (dD) \quad (62)$$

Exploratory tests with this type of thermal-fatigue specimen indicate that all of the major deficiencies of the conventional test method are remedied. The temperature-stress-time variation at the location of failure is easily recorded. The strain can be gaged directly. No effective gage lengths are required in the calculations. Various degrees of restraint can be obtained by varying the thermal length of the specimen. Geometric effects are minimized.

SUMMARY

A modified specimen geometry has been presented that minimizes the difficulties of the conventional thermal-fatigue test. It is suggested that this type of specimen be used as a standard for determining the thermal-fatigue properties of materials. Indications are that this type of test specimen will yield results approximately equal to isothermal strain-fatigue data for materials that have reasonable metallurgical stability.

Tests of tubular specimens should not be abandoned because reliable values of the plastic-strain range and mechanical-strain range can be determined by their use. Methods given in this report for calculating $\Delta\epsilon_p$ and $\Delta\epsilon_m$ for the conventional thermal-fatigue test have considerable utility. Generally the results of thermal-fatigue tests of tubular samples include the effects of the heating method and of geometric instabilities. Tube data are conservative, however, and these results should be considered when reasonable design limits are to be established. The relationship between test data from tubular and solid specimens should be established.

Reports of thermal-fatigue tests should contain a complete description of the material, test conditions, and methods of analysis. The load-temperature graph is the most significant record of the test, and a strong recommendation is presented for its use.

Several methods for calculating the plastic-strain values have been presented. A method for constricting the stress-strain cycle is also given. The slope of this thermal-fatigue stress-strain cycle shows good agreement to the isothermal modulus at the mean temperature.

A need exists to establish a criterion for thermal fatigue that is related to the stress-temperature-time variation of the application and of the material constants α , E, K, N, C, and λ .

ACKNOWLEDGMENTS

The analysis presented in this report was, in part, performed at the University of Alabama for a research project supported by the Metals and Ceramics Division of the Oak Ridge National Laboratory. Appreciation is expressed for this support and to the members of the Division who have assisted and guided this work.

APPENDIX A



Description of the Conventional Thermal-Fatigue Test

Many of the thermal-fatigue-test apparatus described in the literature¹⁶⁻¹⁹ are essentially the same as that designed by Coffin,¹⁶ although certain modifications have appeared.²¹⁻²² A cross section of the Coffin-type test apparatus and a typical specimen design are shown in Figs. 18 and 19. One arrangement of the test apparatus and control system is shown in Fig. 20. The wall thicknesses of the tubular specimens have ranged from 0.010 to 0.137 in.;¹⁶⁻²¹ however, one investigator²² used a solid specimen having a reduced section diameter of 0.190 in.

A large electric current passing through the specimen has been the common heating method,^{16-20,22} although induction heating has been employed²¹ with some accompanying benefit. Cooling has been accomplished by passing a compressed gas¹⁶⁻²⁰ or a cryogenic liquid²¹ through a central hole, or by conduction of the heat through the ends of a solid specimen.²²

The test apparatus shown in Fig. 18 provides a means for anchoring a specimen securely at each end to a massive end plate. The end

¹⁶L. F. Coffin, Jr., Trans. ASME 76, 931-49 (1954).

¹⁷F. J. Mehringer and R. P. Felgar, Trans. ASME, Ser D: J. Basic Eng. 82, 661-70 (1960).

¹⁸A. E. Carden and J. H. Sodergren, "The Failure of 304 Stainless Steel by Thermal-Strain Cycling at Elevated Temperature," paper presented at the ASME Annual Meeting, November 26-December 1, 1961, 61-WA-200 (1961).

¹⁹K. E. Horton and R. S. Stewart, Final Report. Thermal-Stress-Fatigue Behavior of Zirconium and Zirconium Alloys, ATL-A-127 (October 31, 1961).

²⁰H. Majors, Jr., Trans. ASM 51, 421-32 (1959).

²¹E. B. Wylie, C. Hoggatt, and R. Venuti, The Effects of Thermal Cycling Between Cryogenic and Elevated Temperatures on the Mechanical Properties of Materials, DRI-1576-FR, University of Denver (March 15, 1961).

²²F. J. Clauss and J. W. Freeman, Thermal Fatigue of Ductile Materials, Part I, Effect of Temperature Cycle on the Thermal-Fatigue Life of S-816 and Inconel 550, NACA-TN-4160 (September 1958).

UNCLASSIFIED
ORNL-LR-DWG 71548

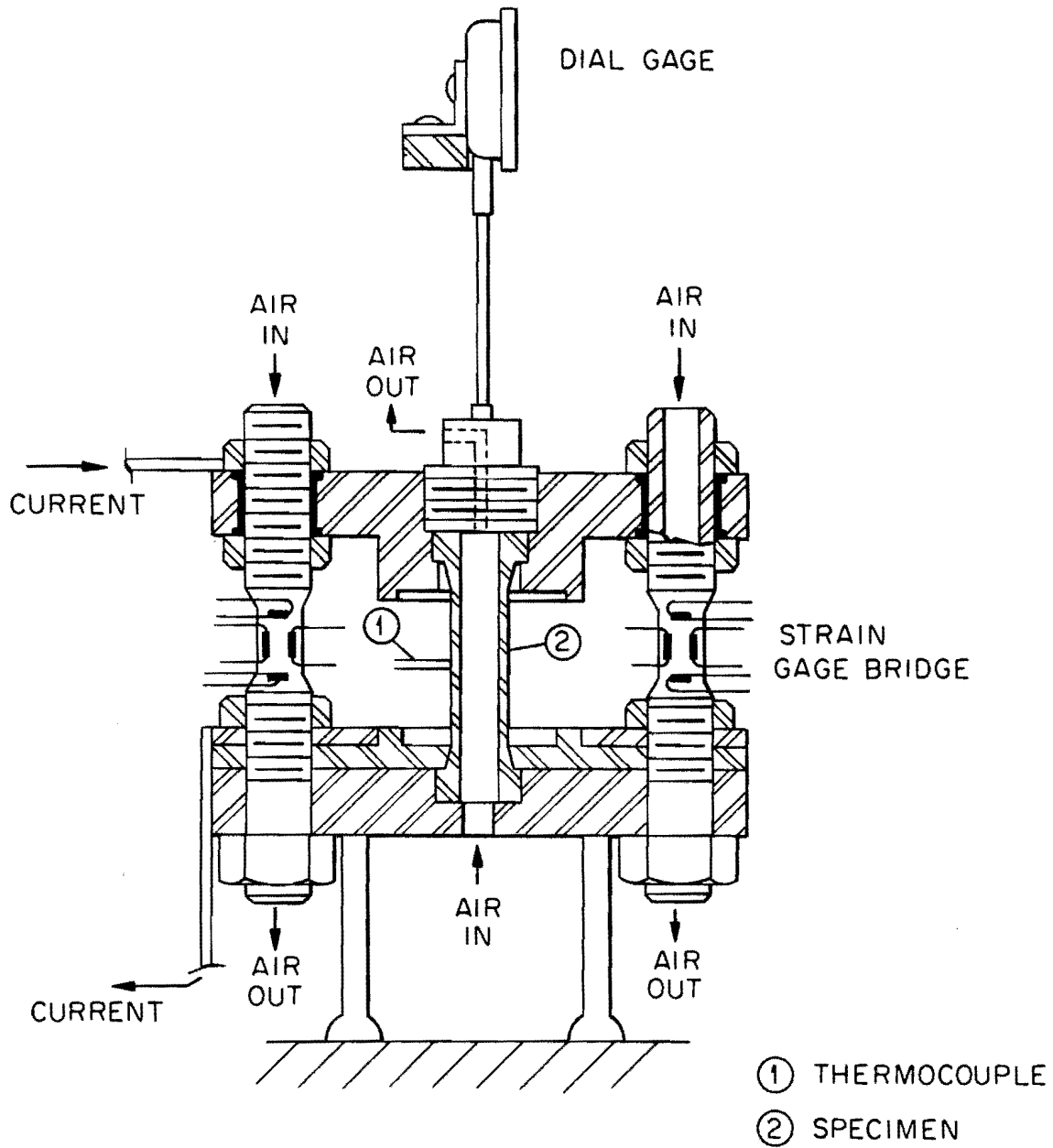


Fig. 18. Thermal-Fatigue Test Apparatus.

UNCLASSIFIED
ORNL-LR-DWG 71549

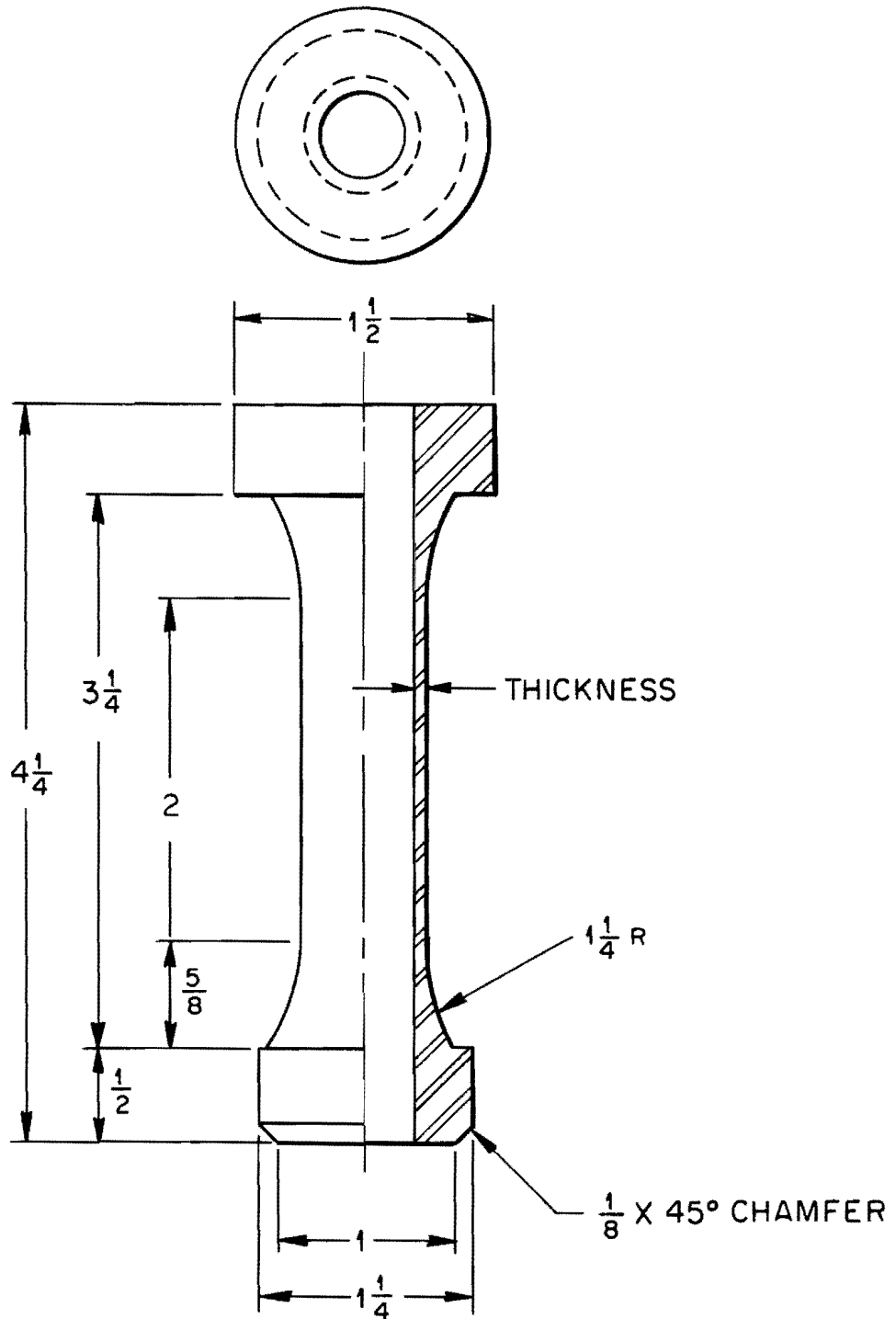


Fig. 19. A Typical Thermal-Fatigue Specimen. (All dimensions are in inches.)

UNCLASSIFIED
PHOTO 61-WA-200

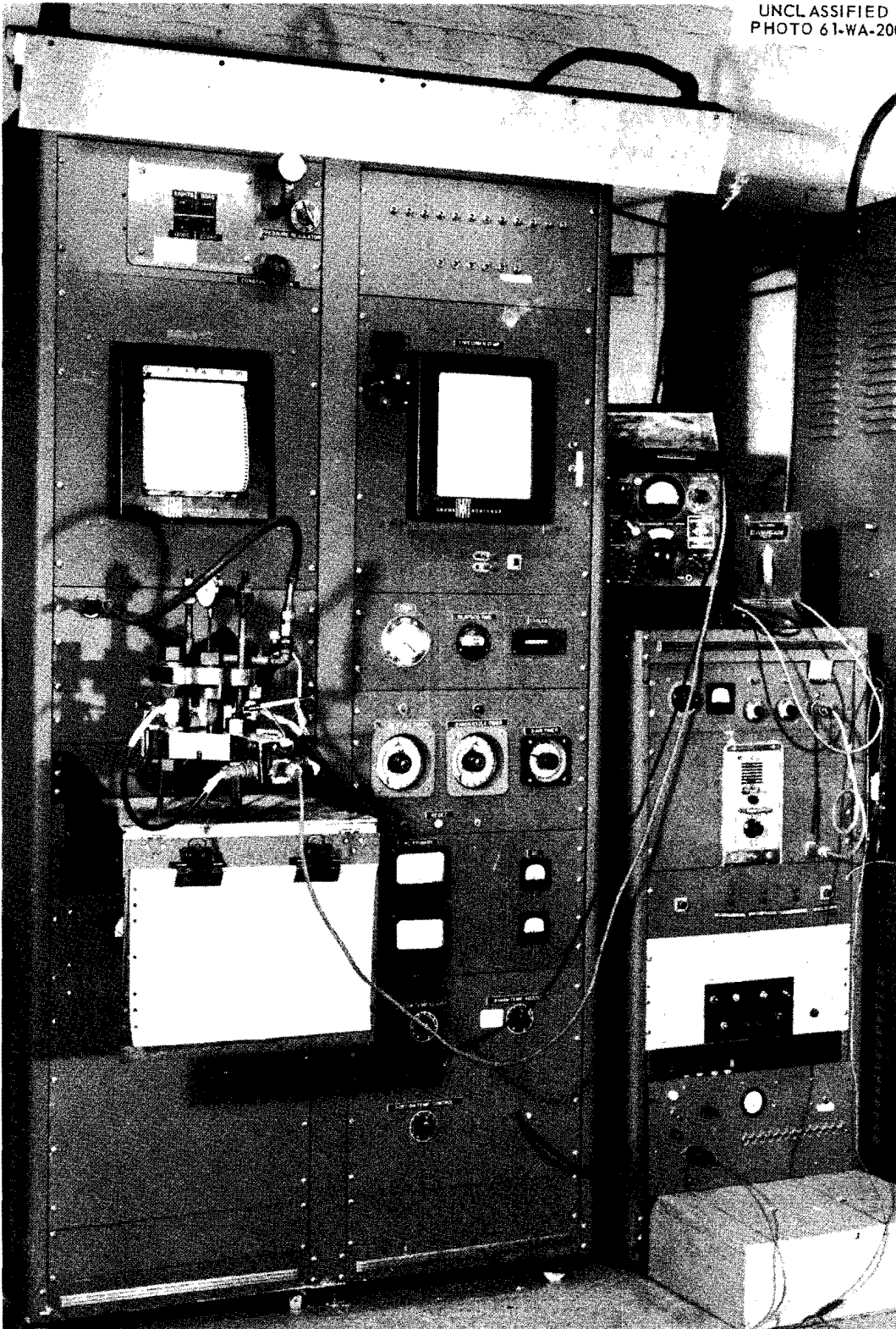


Fig. 20. Conventional Thermal-Fatigue Test Assembly.

plates are connected mechanically, but not electrically, by two stiff load-cell columns. On each load cell, one nut above and one nut below the upper end plate clamp the restraint system together. The restraint system prohibits longitudinal thermal movement of the specimen. The locking nuts can be loosened to allow measurement of the unrestrained thermal movement of the specimen. The longitudinal temperature distribution, or temperature profile, of the specimen is nonuniform, generally parabolic. The large massive ends and specimen fillets constitute an ample heat sink to reduce the temperature of the ends of the gage length. The temperature is measured by a minute thermocouple spot welded to the specimen surface at midlength. The effect of this weld on the specimen surface is generally assumed to be negligible.

For conduction or resistance heating, the heating rate can be controlled by varying the voltage across the specimen. As the temperature increases, heat is dissipated at a greater rate from the specimen and the resistance of the specimen increases. Thus, for constant voltage, the heating rate decreases with increasing temperature. The heating rates commonly have not been controlled. As the specimen temperature is increased, the voltage across the specimen must be increased if the heating rate is to be constant.

Cooling produced by blowing compressed gas through the specimen is also ordinarily nonlinear because the temperature of the gas is constant. As the temperature difference between the specimen and the gas decreases, the cooling rate decreases. Unless the gas reservoir is large, lengthy cooling times reduce the supply pressure, further decreasing the cooling rate. Therefore, in the conventional test, the rates of heating and cooling are not constant and are not truly controlled. Although results of considerable utility can be obtained from the conventional test, some means of control of the heating and cooling rates must be employed if it is necessary to duplicate the temperature-time cycle of the service application in a laboratory test.

Some of the controls that alternate the heating and cooling periods are designed for constant specimen voltage with constant time for heating or cooling.¹⁹ Other designs employ recorder-controller limit switches to cause cycling of heating or cooling when the specimen reaches preset temperature limits.¹⁸ Some control systems include a hold time at either or both of the temperature extremes.¹⁹ The purpose of the hold time is to simulate the stress-temperature-time cycle of the service application. A typical temperature-time record is shown in Fig. 21.

During the hold time the temperature at the center of the specimen is held constant, but the temperature profile is not. In other words, the transient longitudinal temperature distribution is not equal to the steady-state distribution. When this change in temperature distribution occurs, it should be accounted for.

The load cells generally contain resistance-type strain gages mounted on the columns at a reduced cross section. A calibration constant is obtained for these load cells from room-temperature static tests in a universal testing machine. For thermal-fatigue tests having maximum specimen temperatures above 1000°F, a significant temperature rise, zero drift, and possible calibration drift occur in the load cell.¹⁸ Water-cooled, hollow load cells are recommended as a solution to this problem. The restraint system is composed of the end plates and the load cells. This system is not perfectly rigid and an appreciable error in the calculated strain values can result from assuming it so. Machines of the type shown in Fig. 18 have a stiffness in the order of 1.5×10^6 lb/in. The deflection of the restraint during thermal cycling is usually measured with a 0.0001-in. dial gage and the output of the load cells indicates the load on the specimen.

The specimen is manufactured, inspected, measured, and mounted in the test apparatus. The thermocouple is welded and the control limits are set. Special care must be exercised in mounting the specimen and making electrical connections. The low-voltage power circuit often carries several thousand amperes, and large amounts of heat are generated at joints lacking good mechanical clamping and low electrical resistance.

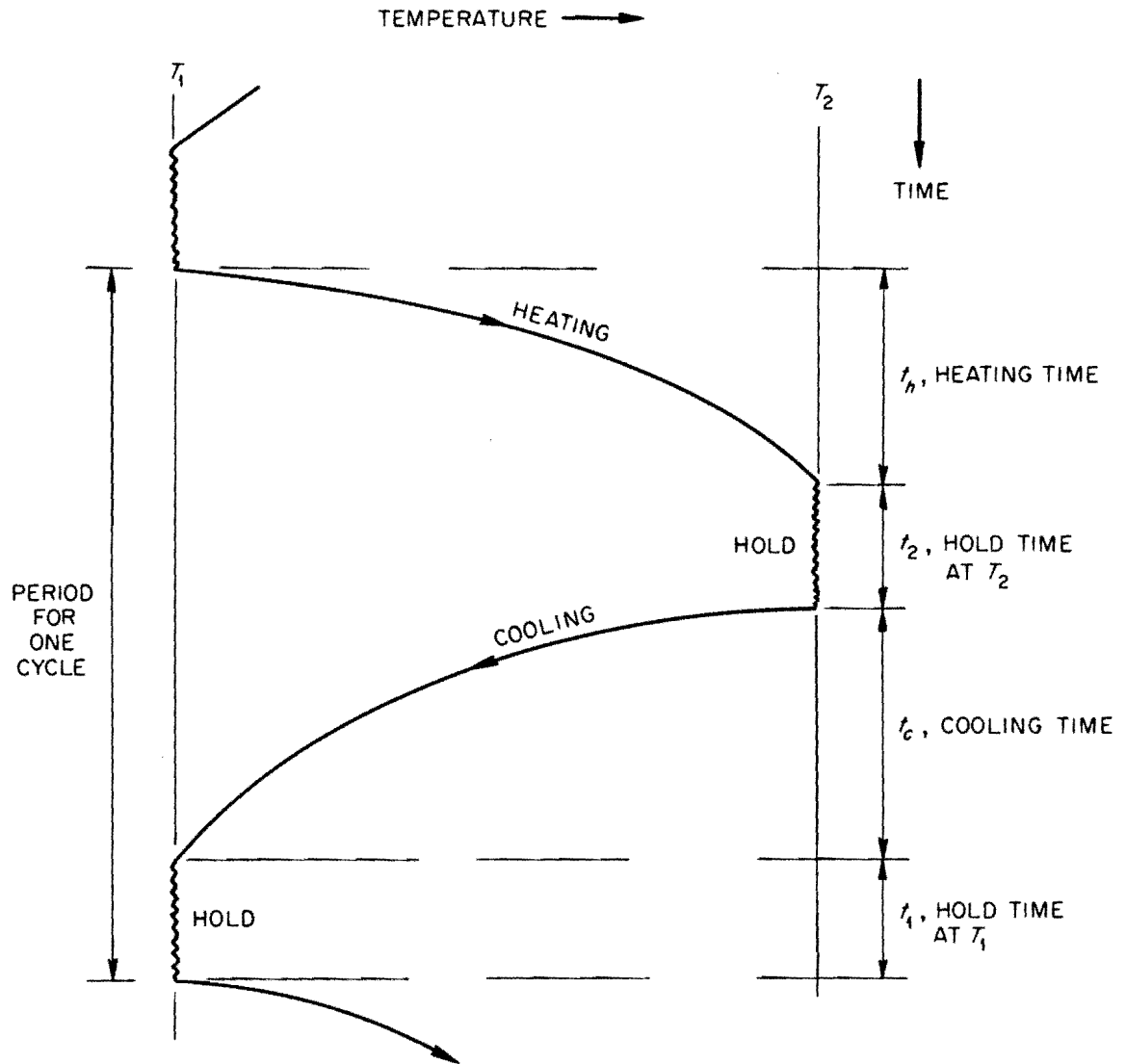


Fig. 21. Typical Temperature-Time Cycle for Thermal-Fatigue Testing.

The total longitudinal thermal movement is determined during a period of uninhibited thermal cycling. Later the cycling is stopped, the temperature is maintained constant (at midrange or one extreme), and the load cells are clamped to the upper end plate by the locking nuts. Special care is taken to ensure against bending of the specimen. The cycle controller is turned on again and the specimen is thermally cycled in a constrained condition; a counter records the number of oscillations. The cycling continues automatically until failure occurs.

The definitions of failure are somewhat arbitrary and are not equivalent. Some of the definitions found in the literature are: (1) complete fracture, (2) a crack through the specimen wall, (3) a crack length greater than 50% of the circumference, and (4) an increase of the outside diameter of 4%. The last definition is highly dependent on specimen geometry and hardly represents a failure of the material. A consistent and explicit definition of failure should be established.

Discussion of the Major Difficulties of the Thermal-Fatigue Test

Perhaps the foremost deficiency of the thermal-fatigue test is the parabolic longitudinal temperature distribution. The plastic behavior of most materials is temperature dependent; consequently, the plastic-strain distribution in the specimen is related to the temperature profile. Too, at elevated temperature the plastic-strain distribution is difficult to measure directly. Moreover, if the plastic-strain distributions for heating and cooling are different, the mean strain will not be zero. Geometric instabilities stem from this distribution inequality in strain, resulting in a change in the conditions of the test. Nearly all investigators have, for some conditions, observed bulging, changes in wall thickness, or both. For resistance-heated specimens, any change of the wall thickness produces a change in the longitudinal temperature distribution. Too, a local thermal gradient is present at the tip of a fatigue crack in a resistance-heated specimen. This thermal disturbance increases the local value of cyclic plastic strain and alters the crack propagation rate.

Other perplexities of the thermal-fatigue test include: (1) the effect of the thermal gradient in the radial direction of the tube, (2) the quenching effect of the cold gas on the surface of the specimen, (3) the effect of the lack of accurate control of the heating and cooling rates, (4) the effect of the lack of uniformity of surface finish, (5) the effect of the large surface-to-volume ratio for the tubular-type specimen, (6) the effect of environment, (7) the effect of strain hardening, strain softening, or relaxation, (8) the effect of metallurgical changes, (9) the effect of the temperature dependence of the mechanical and thermal properties, and (10) the effect of the tensile stress always occurring at the minimum temperature.

These uncertainties, which often constitute objections to the thermal-fatigue test, should not be the sole basis for judging the value of the results. Many of the effects listed are not peculiar to the laboratory test, but must be considered for any structure sustaining cyclic-thermal loading. The severity of these difficulties is not sufficient to prevent an adequate description of material behavior in thermal fatigue. It is necessary, however, that investigators supply with their data a thorough description of their test conditions and test methods. A suggested list of the necessary information is included in Appendix C.



APPENDIX B



Nomenclature

- A - cross-sectional area, square in.
C - constant = $\epsilon_f/2$
K, n - constants of the equation $\epsilon_p = K\sigma^n$
D - dial gage reading, in.
E - modulus of elasticity, psi
F - degree of constraint factor
L - length, in.
N - cycle number
P - load, lb
R - radius, in.
W - energy, in.-lb or in.-lb/in.³
ROA - reduction of area, %
T - temperature, °F
t - time, sec
 δ - total strain, in.
 ϵ - unit strain, dimensionless
 σ - unit stress, psi
 λ - relaxation constant, $\sigma = \sigma_0 e^{-\lambda/t}$
 α - coefficient of thermal expansion, per °F

Subscripts

- g - geometric strain, lineal displacement
m - mechanical strain, sum of elastic and plastic components
e - elastic strain, recoverable
p - plastic strain, nonrecoverable
T - thermal strain
s - spring representing restraint system
f - designation of failure
o - designation of the value at zero load
x, r, z - coordinate directions
t - tensile value
c - compressive value

Superscripts

- deg, ° - designates value for unrestrained cycling
prime, ' - designates value for restrained cycling



APPENDIX C



Required Test Information for the Thermal-Fatigue Test

- I. Material
 - A. Chemical Analysis
 - B. Metallographic Analysis
 - 1. Grain Size
 - 2. Preferred orientation (for anisotropic materials)
 - 3. Phases and precipitates
 - C. Fabrication History
 - D. Properties vs Temperature
 - 1. Coefficient of thermal expansion
 - 2. Modulus of elasticity
 - 3. Constants from isothermal tensile-test data
 n , K , σ_{ys} , σ_{ult} , $el.$, ROA
 - 4. Relaxation, creep, and stress-rupture constants
 - 5. Resistivity
- II. Specimen
 - A. Geometry. Include drawing with dimensions and tolerances.
 - B. Surface Finish and Cleaning
- III. Testing Machine. Include drawing.
 - A. Axiality
 - B. Clamping
 - 1. Description of method
 - 2. Method of prevention of bending
 - C. Load Cells. Include drawing.
 - 1. Calibration constant; tension and compression
 - 2. Frequency of calibration
 - 3. Sensitivity of reading
 - 4. Maximum operating temperature of load cell during any test
 - D. Rigidity
 - 1. Spring constant, lb/in.
 - 2. Graph of load-cell output vs deflection
- IV. Test Conditions
 - A. Environment

B. Temperature

1. Thermocouple material, source, and size
2. Method of attachment
3. Method and frequency of calibration of temperature-indicating system
4. Record of typical temperature vs time
5. Method of heating and control
6. Method of cooling and control
7. Typical longitudinal temperature profile at the maximum and minimum temperature
8. Alteration of profile during test
9. Plot of dial gage vs temperature-free cycling

C. Clamping

1. At maximum, mean, or minimum temperature
2. First half cycle in tension or compression

D. Failure

1. Definition
2. Detection
3. Method of counting cycles

V. Posttest Examination

A. Properties

1. Tensile
2. Metallographic
3. Other

VI. General Information Regarding Data (see Figs. 22 and 23)

A. Method of Determining σ - ϵ Loop

B. Method of Determining P-T Loop

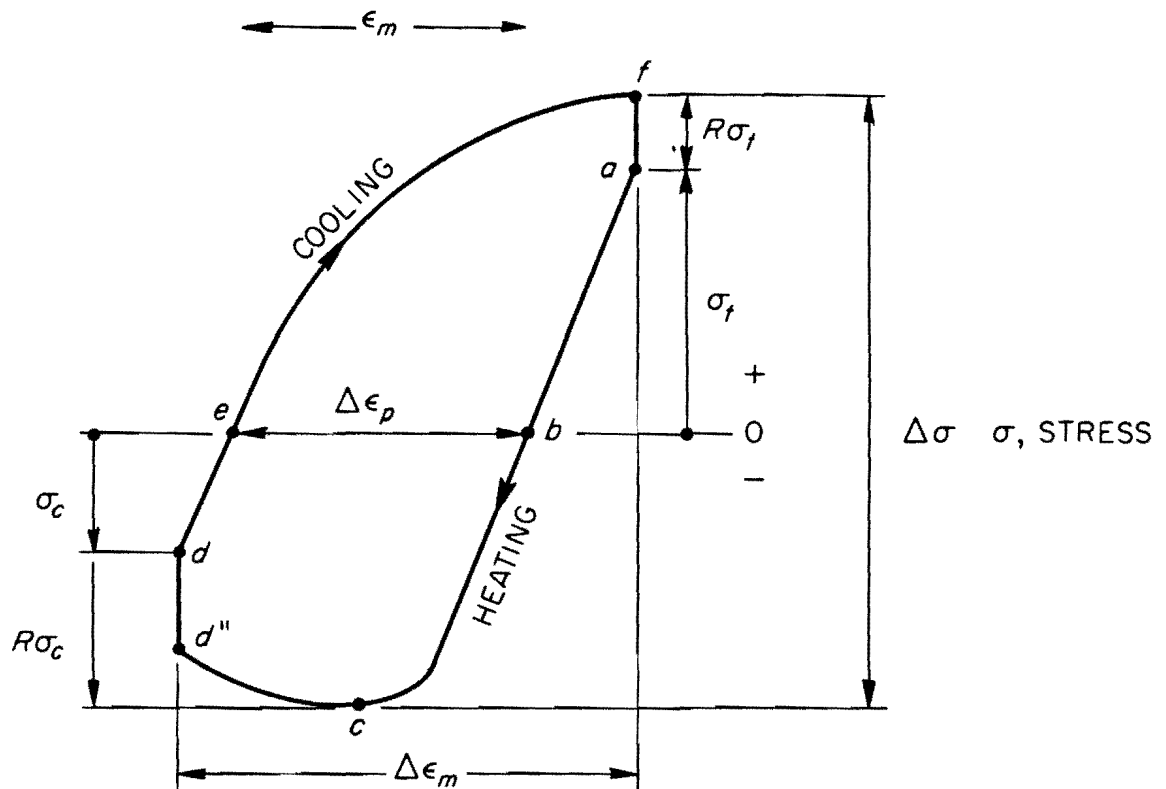
1. Number of loops taken per test

C. Method of Determining $\Delta\epsilon_p$

D. Definition of Test Parameters

1. Initial value
2. Average value
3. Asymptotic value

E. Method of Determining Effective Gage Lengths



CYCLE REGIONS

$a-d''$ HEATING

$d''-d$ HOLD TIME AT T_{MAX}

$d-f$ COOLING

$f-a$ HOLD TIME AT T_{MIN}

$\Delta\sigma$ - MAXIMUM EXTERNAL HEIGHT OF LOOP

σ_f - TENSILE STRESS AT INITIATION OF HEATING

σ_c - COMPRESSIVE STRESS AT INITIATION OF COOLING

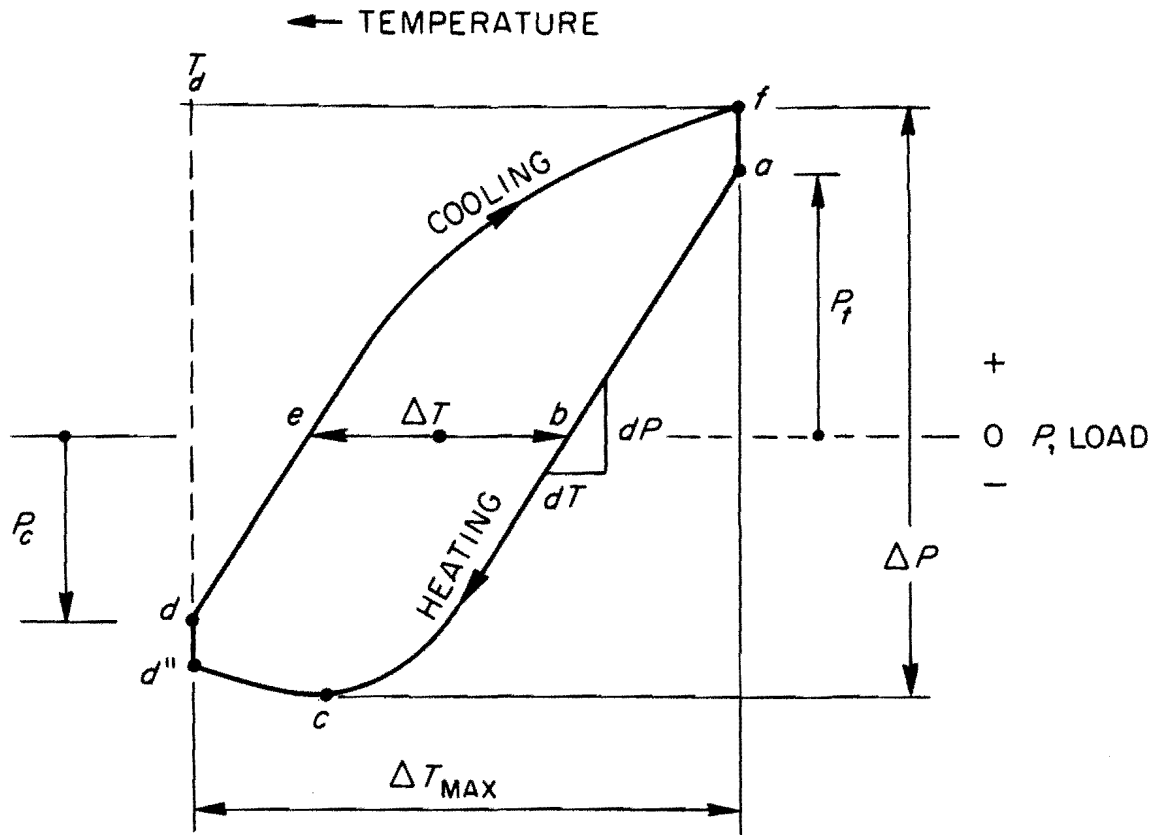
$R\sigma$ - DECREMENT OF STRESS FROM MAXIMUM VALUE

$\Delta\epsilon_m$ - MAXIMUM EXTERNAL WIDTH OF LOOP

$\Delta\epsilon_p$ - MAXIMUM INTERNAL WIDTH OF LOOP

Fig. 22. Stress-Strain Loop.

UNCLASSIFIED
ORNL-LR-DWG 71564



PLASTIC STRAIN RANGE $\Delta\epsilon_p = \alpha(\Delta T_0) \frac{L^0}{L^1}$

MECHANICAL STRAIN RANGE $\Delta\epsilon_m = \alpha(\Delta T_{MAX}) \frac{L^0}{L^1} - \frac{\Delta P}{K_s L^1}$

PLASTIC STRAIN ENERGY PER CYCLE $\Delta E_p = [\int P(dT)] \alpha L^0$

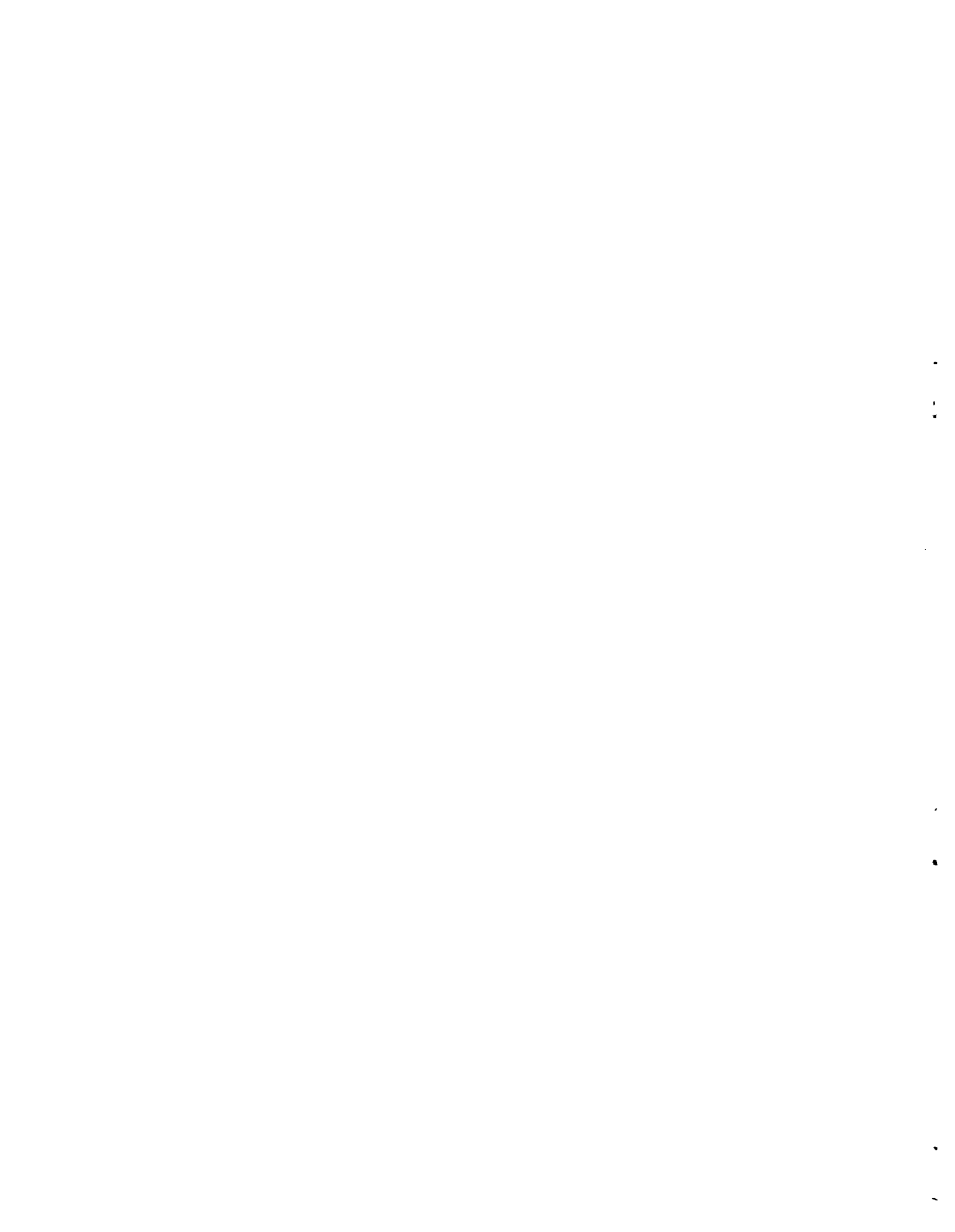
TENSILE STRESS RANGE $\Delta\sigma_t = \frac{P_t}{A}$

TOTAL STRESS RANGE $\Delta\sigma = \frac{\Delta P}{A}$

Fig. 23. Load-Temperature Loop.

VII. Tabular Summary of Individual Tests

- A. Specimen Number
- B. Maximum Temperature
- C. Minimum Temperature
- D. Cycles to Failure
- E. Heating Time, t_n
- F. Hold Time at T_{max} , T_2
- G. Cooling Time, t_c
- H. Hold Time at T_{min} , T_1
- I. Tensile Stress, σ_t
- J. Compressive Stress, σ_c
- K. Total Stress Range, $\Delta\sigma$
- L. Plastic-Strain Range, $\Delta\epsilon_p$
- M. Mechanical-Strain Range, $\Delta\epsilon_m$
- N. Total Unrestrained Thermal Strain, ΔD°
- O. Effective Gage Length, L'
- P. Maximum Change in Outside Diameter, $\%$
- Q. Weight Gain in Grams per Square Inch
- R. Degree of Constraint, F
- S. Plastic Strain Energy per Cycle, ΔW_p



DISTRIBUTION

- | | | | |
|--------|-------------------------------|--------|--|
| 1. | Biology Library | 29. | W. D. Manly |
| 2-3. | Central Research Library | 30. | W. R. Martin |
| 4. | Reactor Division Library | 31. | H. E. McCoy, Jr. |
| 5. | ORNL - Y-12 Technical Library | 32. | C. J. McHargue |
| | Document Reference Section | 33. | P. Patriarca |
| 6-10. | Laboratory Records Department | 34. | R. L. Stephenson |
| 11. | Laboratory Records, ORNL RC | 35. | A. Taboada |
| 12. | Patent Office | 36. | W. C. Thurber |
| 13. | G. M. Adamson, Jr. | 37. | J. T. Venard |
| 14. | D. A. Douglas, Jr. | 38-40. | J. R. Weir |
| 15-19. | A. E. Carden | 41. | J. W. Woods |
| 20. | J. E. Cunningham | 42-44. | J. M. Simmons, AEC
Washington, D.C. |
| 21. | C. W. Dollins | 45-59. | Division of Technical
Information Extension
(DTIE) |
| 22. | J. H. Frye, Jr. | 60. | Research and Development
Division (ORO) |
| 23. | B. L. Greenstreet | | |
| 24-26. | M. R. Hill | | |
| 27. | C. R. Kennedy | | |
| 28. | H. G. MacPherson | | |

